PHILOSOPHICAL TRANSACTIONS OF THE ROYAL SOCIETY A MATHEMATICAL, PHYSICAL & ENGINEERING SCIENCES

The Numerical Solution of Certain Integral Equations with Non-Integrable Kernels Arising in the Theory of Crack Propagation and Elastic Wave Diffraction

R. Burridge

Phil. Trans. R. Soc. Lond. A 1969 **265**, 353-381
doi: 10.1098/rsta.1969.0060

THE NUMERICAL SOLUTION OF CERTAIN INTEGRAL EQUATIONS WITH NON-INTEGRABLE KERNELS ARISING IN THE THEORY OF CRACK PROPAGATION AND ELASTIC WAVE DIFFRACTION

By R. BURRIDGE†

The Pennsylvania State University, University Park, Pa. 16802, *U.S.A.*

(*Communicated by R. Stoneley, F.R.S.—Received* 10 *January* 1969)

CONTENTS

An infinite elastic medium is initially at rest in a prestressed state of plane- or anti-plane strain. At time $t = 0$ a plane crack comes into existence which occupies a strip parallel to the y axis and whose width varies in time.

Assuming that the components of the traction are known on the crack surface it is possible to set up an integral equation on the area of the crack for the relative displacement across the crack.

Although the kernel of this integral equation is non-integrable a method is found for discretizing it and a numerical method of solution is carried out.

The results, which in some cases are the solutions of diffraction problems, are presented graphically.

1. Description of the problem

The problem treated in this paper is one arising in seismology from an attempt to describe mathematically the mechanism of earthquakes. Fault-plane studies indicate that most earthquakes consist of a more or less catastrophic slip of the material on one side of a fault plane relative to the material on the other side. If the amount of this relative slip is known as a function of time and position on the fault plane the radiation from such a seismic source may be calculated

† Permanent address: Department of Applied Mathematics and Theoretical Physics, University of Cambridge.

Vol. 265. A. 1163. (Price 17*s.*; U.S. $2.20.) 33 [Published 11 December 1969

by integrating a suitable Green function. It is the purpose of this paper to describe an idealized dynamical model for which such relative motions may be computed.

The problem may be posed at various levels of sophistication. For instance, if we knew the composition and equation of state of the material at the earthquake focus, its state of stress, and its temperature we might ask how the material would fail. Assuming that the material suffers a localized shear failure we would like to know on which surface the failure occurs, how the failure propagates from some region of nucleation on this surface, and what is the amount of slippage as a function of time and position on the fault plane. Stated with this degree of generality the problem is very complex even for homogeneous materials. The next simplest level at which the problem may be posed is to assume that at least we know the surface across which shearing takes place. This is not unreasonable physically since earthquakes are often associated with pre-existing fault planes, planes of weakness where fracture originally occurred in the geologic past. Moreover, it is not unreasonable on the basis of surface traces of faults to assume a planar form for these surfaces. The problem may be put into a mathematical setting if we know the cohesive tractions acting across this plane of weakness as functions (or functionals) of the relative motion and its history. These functions must be such as to allow instability. For instance if the cohesive tractions at a point depend only on the relative slip or velocity of slip at that point we must suppose that once the motion starts these tractions drop to values below those in the initial static state. Possibly this will occur after an initial increase in traction as in Barenblatt's theory of brittle fracture. But even the simplest problem of this type, the case of anti-plane strain, has only partially yielded to analytical techniques (Kostrov 1964*b*) and this only when the region where the cohesive tractions are non-zero is effectively confined to a line, the crack tip. It was my original aim to attack such problems numerically for anti-plane and plane strain but in the present paper I shall be content with an even more idealized situation. I shall assume that not only is the surface of shear failure known but that it is a plane and that we know in advance what the region of slip on this plane is as a function of time. If we also know the cohesive tractions as a function of space and time on the area of slip we may compute numerically what the relative displacement is across the fault plane. We shall, moreover, confine attention to two-dimensional problems. Mathematically this is almost identical to the problem of the diffraction of elastic waves by a crack whose size may vary in time. So far only self-similar two- and three-dimensional problems of this type have been solved analytically. (See Broberg (1960), Burridge & Willis (1969), Craggs (1966), and Kostrov (1964*a*).) Anything more complicated leads to unwieldy expressions and is best solved numerically. Recently Halliday (1969) has used Kostrov's analysis (Kostrov 1964*b*) to obtain numerically the stresses beyond the crack tips for the second problem considered in §6 of this paper. As Kostrov remarks, it is necessary to supplement the analysis with computational methods in order to carry the solution further than a very limited region.

Previous workers on earthquake mechanisms have usually been content to postulate the relative displacement across the fault plane as a function of time and space with the result that it is sometimes doubtful whether these displacements could arise from any dynamical processes which might govern the focal mechanism. Other workers have simulated the source by means of given distributions of body forces but this again is subject to the same criticism. (See, for instance, Ben-Menahem (1961) and Hirasawa & Stauder (1965).)

Although we do not know the stress field at an earthquake focus and although we do not know what precise form the stress drop may take, at least we shall obtain sources governed by dynamical processes of a fairly plausible kind.

Archambeau (1968) has recently considered realistic models consisting of a moving zones of melting in a prestressed solid and has obtained some numerical results relating to radiation from his sources. His paper should be referred to also for its very full bibliography.

2. The mathematical formulation of the problem

Although the specific numerical solutions obtained later are all for two-dimensional problems, I shall here set up the general three-dimensional scheme. Let x, y, z be Cartesian coordinates and t the time. Let two identical isotropic half-spaces occupy the regions $z > 0$ and $z < 0$. Initially, the system is strained under a stress field which is not purely hydrostatic and the whole system is held in equilibrium by 'frictional' tractions acting across the plane $z = 0$.

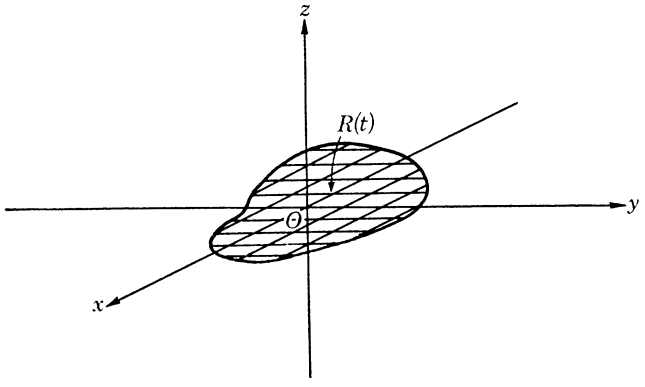

Figure 1. This shows the crack region $R(t)$ lying in the plane $z = 0$. $R(t)$ is a growing region which can support reduced tangential tractions only.

At time $t = 0$ a crack comes into existence and thereafter occupies a region $R(t)$ of the plane $z = 0$. The crack is defined by the fact that on $R(t)$ the shear tractions fall below their initial values (see figure 1). We shall suppose this drop in traction is known as a function of time and position on $R(t)$. Let us denote the initial values of the shear traction with which the material in $z > 0$ acts on the material in $z < 0$ by $\tau_i^0(x, y)$, $i = x, y$ and the values of the corresponding components on $R(t)$ by $\tau_i^R(t, x, y)$. Then we shall regard each of τ_i^0 and τ_i^R as known in advance and hence also their difference τ_i is known:

$$\tau_i(t, x, y) = \tau_i^0(x, y) - \tau_i^R(t, x, y). \tag{2.1}$$

This drop in shear traction allows the possibility of slippage of the material in $z > 0$ relative to the adjacent material in $z < 0$ within the region $R(t)$. However, outside $R(t)$ we shall suppose the material to be welded across the surface $z = 0$.

The problem before us, then, is to find the amount of slip in $R(t)$ as a function of t, x, y. The initial stress field is supposed to have a compressive component so that there is no opening of the crack. This implies that there is no normal *relative* displacement across the crack surface.

Let u_x, u_y, u_z be the x, y, z components of displacement measured relative to the initial equilibrium state, which is not stress-free. For fixed t, x, y it is easy to see that u_x, u_y are odd functions of z and u_z is an even function of z. This implies that on $z = 0$ and off $R(t)$, $u_x = 0$ and $u_y = 0$. Also the drop in the zz-component of stress from its initial value is an odd function of z so that it is zero everywhere on the plane $z = 0$, by continuity.

With this symmetry in mind we need only consider the half-space $z > 0$. Let ρ, λ, μ be the density and Lamé constants of the elastic material. Then we need to solve the following problem.

In $z > 0$

$$\left.\begin{aligned} \rho \frac{\partial^2 \boldsymbol{u}}{\partial t^2} &= (\lambda+\mu)\,\nabla(\nabla.\boldsymbol{u}) + \mu\nabla^2\boldsymbol{u}, \\ \boldsymbol{u} &= 0 \quad \text{for} \quad t < 0, \end{aligned}\right\} \tag{2.2}$$

where $\boldsymbol{u} = (u_x, u_y, u_z)$.

On $z = 0$ the z component of the drop in traction is zero;

$$-\lambda\nabla.\boldsymbol{u} - 2\mu\frac{\partial u_z}{\partial z} = 0 \quad \text{everywhere.} \tag{2.3}$$

On the region $R(t)$ of $z = 0$ the x- and y-traction drops are prescribed so that

$$\left.\begin{aligned} -\mu\left(\frac{\partial u_x}{\partial z} + \frac{\partial u_z}{\partial x}\right) &= \tau_x(t,x,y), \\ -\mu\left(\frac{\partial u_y}{\partial z} + \frac{\partial u_z}{\partial y}\right) &= \tau_y(t,x,y). \end{aligned}\right\} \tag{2.4}$$

Off $R(t)$, but still in the plane $z = 0$,

$$u_x = 0, \quad u_y = 0. \tag{2.5}$$

If τ_x, τ_y and $R(t)$ are given it is required to find u_x and u_y on $R(t)$

The method of solution is to set up a linear integral equation on the plane $z = 0$ for u_x, u_y, u_z. Such a formulation has been used by Banaugh (1962) and by Banaugh & Goldsmith (1963) for the numerical solution of problems involving the diffraction of harmonic elastic waves by obstacles of various shapes and also by Friedman & Shaw (1962) for time-dependent acoustic diffraction problems.

Having found the numerical formulation of this equation we may eliminate u_z and so set up an integral equation for u_x, u_y alone. However, our method of discretizing the kernel is such that we must obtain the kernel for the first integral equation before eliminating u_z.

I shall now outline the general theoretical scheme for the method and in §4 explain in detail how the integral equation is discretized for antiplane strain. In §7 the discretization for plane strain is described.

Denote by R the region of t, x, y in which (x, y) lies in $R(t)$. Let τ_x, τ_y, τ_z denote the x-, y-, z-components of the drop in traction on $z = 0$ and u_x, u_y, u_z the x, y, z components of displacement on $z = 0$. (At this stage we do not require τ_z to be zero.) Suppose that u_x, u_y, u_z are known as functions of t, x, y then τ_x, τ_y, τ_z depend linearly upon u_x, u_y, u_z. Since this linear dependence is translationally invariant in t, x, y we may write it as a convolution

$$\boldsymbol{\tau} = \boldsymbol{K} * \boldsymbol{u}, \tag{2.6}$$

where $\boldsymbol{\tau} = (\tau_x, \tau_y, \tau_z)$, $\boldsymbol{K}$ is a 3×3 matrix whose elements are distributions in t, x, y and $*$ stands for convolution in t, x, y. Thus (2.6) may be written more explicitly as

$$\tau_i(t,x,y) = \int_C \mathrm{d}t'\,\mathrm{d}x'\,\mathrm{d}y' K_{ij}(t-t', x-x', y-y')\,u_j(t', x', y'), \tag{2.7}$$

where $i, j = x, y, z$. From consideration of domains of dependence the region C of integration is defined by

$$(x-x')^2 + (y-y')^2 \leqslant \alpha^2(t-t')^2 \quad (t' < t), \tag{2.8}$$

where $\alpha = \sqrt{([\lambda+2\mu]/\rho)}$, the P wave velocity.

If we now take into account (2.2) to (2.5), (2.7) becomes

$$\begin{aligned}\tau_x(t,x,y) = &\int_{C\cap R} K_{xx}(t-t',x-x',y-y')\,u_x(t',x',y')\,\mathrm{d}t'\,\mathrm{d}x'\,\mathrm{d}y' \\ &+\int_{C\cap R} K_{xy}(t-t',x-x',y-y')\,u_y(t',x',y')\,\mathrm{d}t'\,\mathrm{d}x'\,\mathrm{d}y' \\ &+\int_{C} K_{xz}(t-t',x-x',y-y')\,u_z(t',x,'y')\,\mathrm{d}t'\,\mathrm{d}x'\,\mathrm{d}y; \end{aligned} \tag{2.9}$$

a similar equation with $\tau_x, K_{xx}, K_{xy}, K_{xz}$ replaced by $\tau_y, K_{yx}, K_{yy}, K_{yz}$;

and

$$\begin{aligned}0 = &\int_{C\cap R} K_{zx}(t-t',x-x',y-y')\,u_x(t',x',y')\,\mathrm{d}t'\,\mathrm{d}x'\,\mathrm{d}y' \\ &+\int_{C\cap R} K_{zy}(t-t',x-x',y-y')\,u_y(t',x',y')\,\mathrm{d}t'\,\mathrm{d}x'\,\mathrm{d}y' \\ &+\int_{C} K_{zz}(t-t',x-x',y-y')\,u_z(t',x',y')\,\mathrm{d}t'\,\mathrm{d}x'\,\mathrm{d}y'. \end{aligned} \tag{2.10}$$

The reason for the difference between the domain of integration in the third integrals in (2.9) and (2.10) is that whereas $u_x = 0$, $u_y = 0$ outside R, u_z is not necessarily zero there.

The equations (2.9) and (2.10) are sufficient to determine u_x, u_y on R and u_z everywhere on $z = 0$ provided that we can find discretizations of the kernels K_{ij}.

It turns out that not only are the analytic expressions for $\boldsymbol{K}$ extremely unwieldy but they are regularizations of non-integrable functions. Thus at first sight it is not clear how to approximate them numerically. However, the method of discretization discussed in § 4 below does not require that the analytic forms of K_{ij} should be known, nor does the non-integrability impair the method.

Let us rewrite (2.7) in the form

$$\tau_x = K_{xx} * u_x + K_{xy} * u_y + K_{xz} * u_z, \tag{2.11}$$

$$\tau_y = K_{yx} * u_x + K_{yy} * u_y + K_{yz} * u_z, \tag{2.12}$$

$$0 = K_{zx} * u_x + K_{zy} * u_y + K_{zz} * u_z. \tag{2.13}$$

If we now let $K_{zz}^{-1}(t,x,y)$ be the kernel inverse to $K_{zz}(t,x,y)$, that is

$$K_{zz}^{-1} * \tau = w \quad \text{whenever} \quad \tau = K_{zz} * w, \tag{2.14}$$

we may solve (2.13) for u_z and so eliminate u_z from (2.11) and (2.12).

The resulting equations are

$$\tau_x = (K_{xx} - K_{zz}^{-1} * K_{xz} * K_{zx}) * u_x + (K_{xy} - K_{zz}^{-1} * K_{xz} * K_{zy}) * u_y, \tag{2.15}$$

$$\tau_y = (K_{yx} - K_{zz}^{-1} * K_{yz} * K_{zx}) * u_x + (K_{yy} - K_{zz}^{-1} * K_{yz} * K_{zy}) * u_y. \tag{2.16}$$

The advantage of this form over (2.11) to (2.13) is not only that u_z need not be determined but that u_x, u_y are zero outside R and so the convolution integrals may be limited to integrals over R with a great saving of computer time (see § 10).

In what follows only two-dimensional forms of the problem are solved in which all functions are independent of y and only one of u_x, u_y are non-zero. In principle a similar method would apply almost as easily to three-dimensional problems but the computer time and space required would be much greater.

PHILOSOPHICAL TRANSACTIONS OF THE ROYAL SOCIETY A MATHEMATICAL, PHYSICAL & ENGINEERING SCIENCES

3. The integral equation for anti-plane strain

In order to simplify the expressions let us choose units of length and time so that the shear wave speed $\beta = \sqrt{(\mu/\rho)}$ is unity and the unit of mass so that the density of the material is unity.

Suppose that $R(t)$ is a strip parallel to the axis of y and that u_y depending only on t, x, z is the only non-zero component of displacement.

The equation to be satisfied by u_y in the half space $z > 0$ is

$$\frac{\partial^2 u_y}{\partial t^2} - \frac{\partial^2 u_y}{\partial x^2} - \frac{\partial^2 u_y}{\partial z^2} = 0. \tag{3.1}$$

On $z = 0$ in R the stress drop is prescribed:

$$-\frac{\partial u_y}{\partial z} = \tau_y \quad \text{in} \quad R, \tag{3.2}$$

where τ_y is given. On $z = 0$ but outside R

$$u_y = 0. \tag{3.3}$$

The problem is to find u_y on R.

It is customary in such problems to solve first for $\tau_y = -\partial u_y/\partial z$ outside R. Having found τ_y outside R, τ_y is then known everywhere on $z = 0$ so that u_y may be written down on R in the form

$$u_y(t, x) = \frac{1}{\pi} \int_C \frac{\tau_y(t', x')}{\{(t-t')^2 - (x-x')^2\}^{\frac{1}{2}}} \, dt' \, dx', \tag{3.4}$$

where C is now defined by

$$(x-x')^2 < (t-t')^2 \quad (t' < t). \quad \text{(See Kostrov 1964}b\text{.)}$$

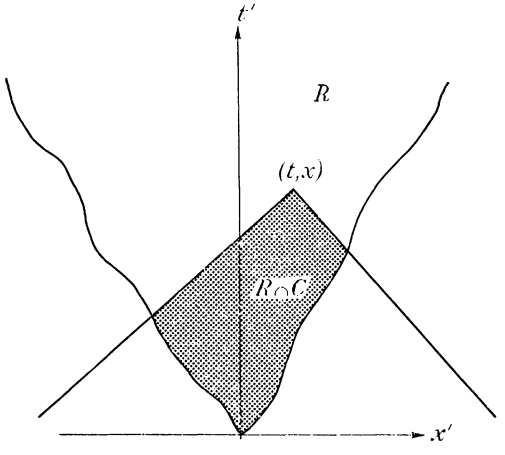

Figure 2. This depicts the region of integration $R \cap C$ hatched in the (t', x')-plane. $R \cap C$ is the intersection of the crack region R with the backward characteristic quarterplane C whose apex is at the point (t, x).

In view of the fact that we wish to apply a numerical procedure it would be convenient if we could limit attention to the region R without having to calculate τ_y outside R.

But we can invert (3.4) to get

$$\tau_y(t, x) = \frac{1}{\pi} \int_{R \cap C} \frac{u_y(t', x')}{\{(t-t')^2 - (x-x')^2\}^{\frac{3}{2}}} \, dt' \, dx', \tag{3.5}$$

where the function $1/\pi\{(t-t')^2-(x-x')^2\}^{\frac{3}{2}}$ must be considered as a regularization and corresponds to K_{yy} of § 2 (see figure 2). Since $u_y = 0$ outside R we have limited the domain of integration to R.

We shall now describe how this non-integrable kernel may be discretized.

4. The discretization of the kernel

We may write

$$-\left.\frac{\partial u_y}{\partial z}\right|_{z=0} = K_{yy} * (u_y|_{z=0}), \tag{4.1}$$

where u_y satisfies (3.1) with zero initial conditions. But $-\partial u_y/\partial z$ also satisfies (3.1) with zero initial conditions so that

$$\left.\frac{\partial^2 u_y}{\partial z^2}\right|_{z=0} = -\frac{\partial}{\partial z}\left(-\frac{\partial u_y}{\partial z}\right)\Big|_{z=0} = K_{yy} * \left(-\left.\frac{\partial u_y}{\partial z}\right|_{z=0}\right) = K_{yy} * K_{yy} * u_y|_{z=0}. \tag{4.2}$$

Hence from (3.1) we obtain $$K_{yy} * K_{yy} * u_y = \left(\frac{\partial^2}{\partial t^2} - \frac{\partial^2}{\partial x^2}\right) u_y, \tag{4.3}$$

or, $$K_{yy} * K_{yy} * u_y = \{\delta''(t)\,\delta(x) - \delta(t)\,\delta''(x)\} * u_y, \tag{4.4}$$

where δ and δ'' are the Dirac δ and its second derivative. Since (4.4) is true for arbitrary $u_y(t, x)$ we must find K_{yy} such that

$$K_{yy} * K_{yy} = \delta''(t)\,\delta(x) - \delta(t)\,\delta''(x), \tag{4.5}$$

where we have written $u_y(t, x)$ for $u_y(t, x, +0)$. But $\delta''(t)\,\delta(x) - \delta(t)\,\delta''(x)$ is easily discretized by using the usual simple difference schemes for second derivatives.

Table 1. The discretization of $\delta''(t)\,\delta(x)$

i \ j	-1	0	1
0	0	$1/h^2$	0
1	0	$-2/h^2$	0
2	0	$1/h^2$	0

Table 2. The discretization of $\delta(t)\,\delta''(x)$

i \ j	-1	0	1
0	0	0	0
1	$1/h^2$	$-2/h^2$	$1/h^2$
2	0	0	0

Let us now consider a square grid of points in the plane with grid lines parallel to the t and x axes with grid spacing $\Delta t = \Delta x = h$ so that a point (i, j) (i, j integers) corresponds to the values $t = ih$, $x = jh$. With this grid we discretize $\delta''(t)\,\delta(x) - \delta(t)\,\delta''(x)$ by discretizing $\delta''(t)\,\delta(x)$ as the array shown in table 1, and $\delta(t)\,\delta''(x)$ as the array shown in table 2. All other components of these arrays are taken to be zero.

Let us write the discretization of K_{yy} in the form $(1/h)\,\bar{K}$ then (4.5) leads to

$$\sum_i \sum_j \bar{K}(i_0-i, j_0-j)\,\bar{K}(i,j) = H(i_0,j_0), \tag{4.6}$$

where $H(i_0,j_0)$ is the array whose only non-zero elements are

$$H(0,0) = H(2,0) = 1, \quad H(1,1) = H(1,-1) = -1. \tag{4.7}$$

Because of consideration of influence domains $\bar{K}(i,j)$ is restricted to be zero except for $0 \leqslant |j| \leqslant i$. Under these restrictions, by setting $i_0 = 0, j_0 = 0$ in (4.6), we obtain

$$\bar{K}^2(0,0) = H(0,0) = 1. \tag{4.8}$$

Hence $\bar{K}\ (0,0) = \pm 1$. Actually we shall take

$$\bar{K}(0,0) = 1. \tag{4.9}$$

This point will be considered again later. Now set $i_0 = 1, j_0 = 1$ in (4.6) to get

$$\bar{K}(0,0)\,\bar{K}(1,1) + \bar{K}(1,1)\,\bar{K}(0,0) = -1,$$

which implies

$$\bar{K}(1,1) = -0.5. \tag{4.10}$$

Similarly,

$$\bar{K}(1,-1) = -0.5. \tag{4.11}$$

Having found $\bar{K}(i,j)$ for $i < i_0$ we may obtain $\bar{K}(i_0,j_0)$ from

$$2\bar{K}(0,0)\,\bar{K}(i_0,j_0) = H(i_0,j_0) - \sum_{i=1}^{i_0-1} \sum_j \bar{K}(i_0-i, j_0-j)\,\bar{K}(i,j). \tag{4.12}$$

This simple recursive scheme gives the required discretization of the kernel. It turns out that $\bar{K}(i,j)$ takes on non-zero values only when $i+j$ is even and $|j| \leqslant i$. The numerical values for small i,j are given in table 3.

TABLE 3. THE ARRAY $\bar{K}(i,j)$

i \ j	−5	−4	−3	−2	−1	0	1	2	3	4	5
0	0.000000	0.000000	0.000000	0.000000	0.000000	1.000000	0.000000	0.000000	0.000000	0.000000	0.000000
1	0.000000	0·000000	0.000000	0.000000	−0.500000	0.000000	−0.500000	0.000000	0.000000	0.000000	0.000000
2	0.000000	0.000000	0.000000	−0.125000	0.000000	0.250000	0.000000	−0.125000	0.000000	0.000000	0.000000
3	0.000000	0.000000	−0.062500	0.000000	0.062500	0.000000	0.062500	0.000000	−0.062500	0.000000	0.000000
4	0.000000	−0.039063	0.000000	0.031250	0.000000	0.015625	0.000000	0.031250	0.000000	−0.039063	0.000000
5	−0.027344	0.000000	0.019531	0.000000	0.007813	0.000000	0.007813	0.000000	0.019531	0.000000	−0.027344

5. THE NUMERICAL SOLUTION OF THE INTEGRAL EQUATION

The numerical method described here is the straightforward solution of (3.5), replacing integrals by sums in the simplest way.

Let us replace $\tau_y(t,x)$ and $u_y(t,x)$ by $\tau_y(i,j)$ and $u_y(i,j)$ where

$$\tau_y(i,j) = \tau_y(hi, hj) \quad \text{and} \quad u_y(i,j) = u_j(ih, jh). \tag{5.1}$$

Thus as in the thermodynamics literature we use the same name for the same physical quantity irrespectively of what the functional arguments are.

Then (3.5) takes the form

$$\tau_y(i_0,j_0) = 1/h \sum_{(hi,hj)\in R} \sum \bar{K}(i_0-i, j_0-j)\,u_y(i,j). \tag{5.2}$$

Hence
$$\bar{K}(0,0)\,u_y(i_0,j_0) = h\tau_y(i_0,j_0) - \sum_{i>0}\sum \bar{K}(i,j)\,u_y(i_0-i,j_0-j). \tag{5.3}$$

At this point it is possible to determine which sign $\bar{K}(0,0)$ must have. We consider the values of $u_y(i_0,j_0)$ when τ_y and u_y are zero for $i < i_0$ but $\tau_y(i_0,j_0) = 1$, say. It is easy to see that (5.3) reduces to
$$\bar{K}(0,0)\,u_y(i_0,j_0) = h \tag{5.4}$$
and that, since $u_y(i_0,j_0)$ must have the same sign as τ_y,
$$\bar{K}(0,0) = 1. \tag{5.5}$$
Thus if $u_y(i,j)$ is known for $i < i_0$ and $(hi, hj) \in R$, $u(i_0,j_0)$ may be computed.

It is interesting to notice the analogy between this scheme and the integration of a system of first order ordinary differential equations. Notice the step-size enters linearly as it would for a first-order system of differential equations. This is not surprising since we could write equation (4.3) in the form
$$K_{yy} * \equiv \left(\frac{\partial^2}{\partial t^2} - \frac{\partial^2}{\partial x^2}\right)^{\frac{1}{2}}, \tag{5.6}$$
which is homogeneous of order 1 in the derivatives.

Thus the operation of convolution with K_{yy} is the square root of a partial differential operator. In fact the situation is akin to that found in the context of ordinary derivatives of fractional order $\frac{1}{2}$ which may be discretized analogously.

When we come to study the corresponding theory for plane strain we shall meet more complicated algebraic functions of partial differential operators which are homogeneous of order 1. The particular ones we shall meet are solutions of quadratic equations whose coefficients are partial differential operators.

Friedlander (1946) considered a very similar situation from an analytical point of view. See particularly his equations (1.6) to (1.9).

6. Comparison of numerical results with some theoretical calculations

Since the numerical scheme described in § 5 is of a somewhat unusual nature it is desirable to compare the numerical results obtained from its use with analytic calculations where possible.

By a slight extension of Kostrov's method (Kostrov 1964*b*) it is possible to solve (3.5) analytically at least for a limited range of values of t.

It turns out that $u_y(t,x)$ depends only on values of $\tau_y(t',x')$ for (t',x') inside the rectangle I and the quarterplane II as shown in figure 3. The lines bordering I are the characteristics through (t,x) and their reflexions in the boundaries of the region R. These lines are continued to enclose the quarterplane II, part of which lies outside R.

The formula giving $u_y(t,x)$ is
$$u_y(t,x) = \frac{1}{\pi}\int_{\mathrm{I}} \frac{\tau_y(t',x')}{\{(t-t')^2-(x-x')^2\}^{\frac{1}{2}}}\,\mathrm{d}t'\,\mathrm{d}x' - \frac{1}{\pi}\int_{\mathrm{II}} \frac{\tau_y(t',x')}{\{(t-t')^2-(x-x')^2\}^{\frac{1}{2}}}\,\mathrm{d}t'\,\mathrm{d}x'. \tag{6.1}$$
(See Fox (1949) for an alternative approach to a similar problem.)

If the disturbance does not start until $t = 0$ then there will be a range of values of (t,x) for which non-zero values of τ_y in I and II occur only within R as for instance when (t,x) is in A, B, C, or D of figure 4 (see below). In such regions the disturbance may be computed very simply.

Let us solve the following problem. The elastic material is in a uniform state of shear with unit tractions acting across $z = 0$ in the y direction. At $t = 0$ the infinite strip $z = 0$, $-1 < x < 1$ becomes lubricated so that it cannot support any shear tractions. Thus the stress drop

$$\tau_y = 1 \quad \text{on} \quad z = 0, \quad -1 < x < 1, \quad t \geqslant 0.$$

It is easier to solve for $\partial u_y/\partial t$ than to use (6.1) directly for u_y.

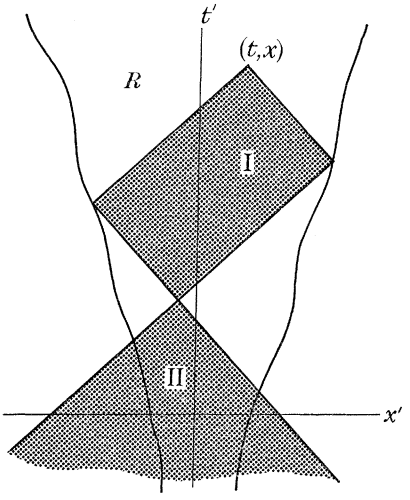

FIGURE 3. The hatched areas are the rectangle I and the quarterplane II which form the region of integration in formula (6.1).

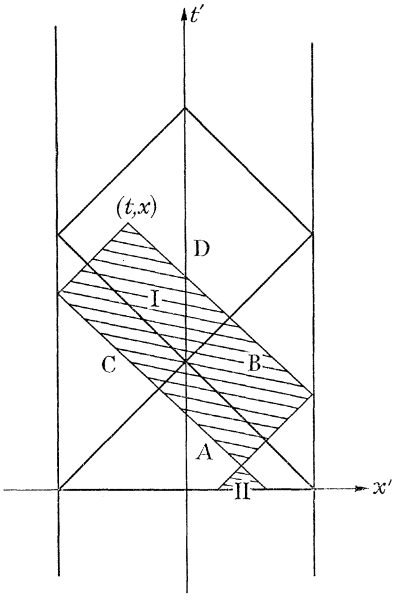

FIGURE 4. The region R corresponding to the solutions in figures 5 to 8 is the infinite strip $t > 0$, $-1 < x < 1$. Regions A, B, C, D are defined by the heavy lines. The shaded regions I and II are shown for (t, x) in D and illustrate the fact that for $t' > 0$ and (t, x) in A, B, C, D, I and II lie within R.

Thus if in (6.1) we replace u_y and τ_y by their time derivatives we obtain

$$\frac{\partial u_y}{\partial t}(t,x) = \frac{1}{\pi}\int_{\mathrm{I}} \frac{\delta(t')\,\mathrm{d}t'\,\mathrm{d}x'}{\{(t-t')^2-(x-x')^2\}^{\frac{1}{2}}} - \frac{1}{\pi}\int_{\mathrm{II}} \frac{\delta(t')\,\mathrm{d}t'\,\mathrm{d}x'}{\{(t-t')^2-(x-x')^2\}^{\frac{1}{2}}} \tag{6.2}$$

for (t, x) in A, B, C, D of figure 4. It is convenient first to evaluate

$$\int_{x-a}^{x+b} \frac{\mathrm{d}x'}{\{t^2-(x-x')^2\}^{\frac{1}{2}}}, \tag{6.3}$$

which is

$$\sin^{-1}\left(\frac{b}{t}\right) - \sin^{-1}\left(\frac{a}{t}\right). \tag{6.4}$$

For (t, x) in A

$$\frac{\partial u_y}{\partial t}(t,x) = \frac{1}{\pi}\int_{x-t}^{x+t} \frac{\mathrm{d}x'}{\{t^2-(x-x')^2\}^{\frac{1}{2}}} = 1. \tag{6.5}$$

For (t, x) in B

$$\frac{\partial u_y}{\partial t}(t,x) = \frac{1}{\pi}\sin^{-1}\left(\frac{2-2x}{t}-1\right) + \tfrac{1}{2}. \tag{6.6}$$

For (t, x) in C

$$\frac{\partial u_y}{\partial t}(t,x) = \frac{1}{\pi}\sin^{-1}\left(\frac{2+2x}{t}-1\right) + \tfrac{1}{2}. \tag{6.7}$$

For (t, x) in D

$$\frac{\partial u_y}{\partial t}(t,x) = \frac{1}{\pi}\left\{\sin^{-1}\left(\frac{2-2x}{t}-1\right) + \sin^{-1}\left(\frac{2+2x}{t}-1\right)\right\}. \tag{6.8}$$

Thus for $x = 0$

$$\frac{\partial u_y}{\partial t} = 1 \quad (0 < t < 1)$$

$$= \frac{2}{\pi}\sin^{-1}\left(\frac{2}{t}-1\right) \quad (1 < t < 3). \tag{6.9}$$

The function $\partial u_y/\partial t$ given in (6.5) to (6.8) is plotted in figure 5. The solution for $\partial u_y/\partial t$ by the numerical scheme of § 5 for the same problem is shown in figure 6.

The numerical solution for u_y itself is shown in figure 7. Here we can compare the numerical solution for $t = 10$ with the static solution, which is

$$u_y = (1-x^2)^{\frac{1}{2}}. \tag{6.10}$$

This is done in figure 9 where the continuous line consists of straight line segments joining the values of the numerical solution for $t = 10$ at grid points in x. The broken line is the function $(1-x^2)^{\frac{1}{2}}$ also plotted as straight line segments joining the points for values of x at grid points.

Figure 8 is another plot of $\partial u_y/\partial t$ with the time scale halved and the vertical scale doubled as compared with figure 6. The overall shape is clearly visible for $3 < t < 10$, whereas some detail for small t is obscured. Notable is the second diffracted wave striking the edge $x = 1$ at $t = 4$. This is scarcely visible in figure 6.

It should be noted that in figures 5 to 9 the grid points in x are mid-points of the twenty intervals $\frac{1}{10}$ unit long in which the interval $-1 < x < 1$ may be divided. The error at $x = \pm 0.05$ is 2.6 %. This error is less than the percentage uncertainty in the crack width in terms of the discretization step size.

It is interesting, though probably not significant, that if we take the edge of the crack to lie not a half-step beyond the last x value but three-quarters the numerical solution for $t = 10$ lies almost exactly on $\{(1.025)^2-x^2\}^{\frac{1}{2}}$, the exact analytic solution for a static crack of width 1.025.

PHILOSOPHICAL TRANSACTIONS OF THE ROYAL SOCIETY A MATHEMATICAL, PHYSICAL & ENGINEERING SCIENCES

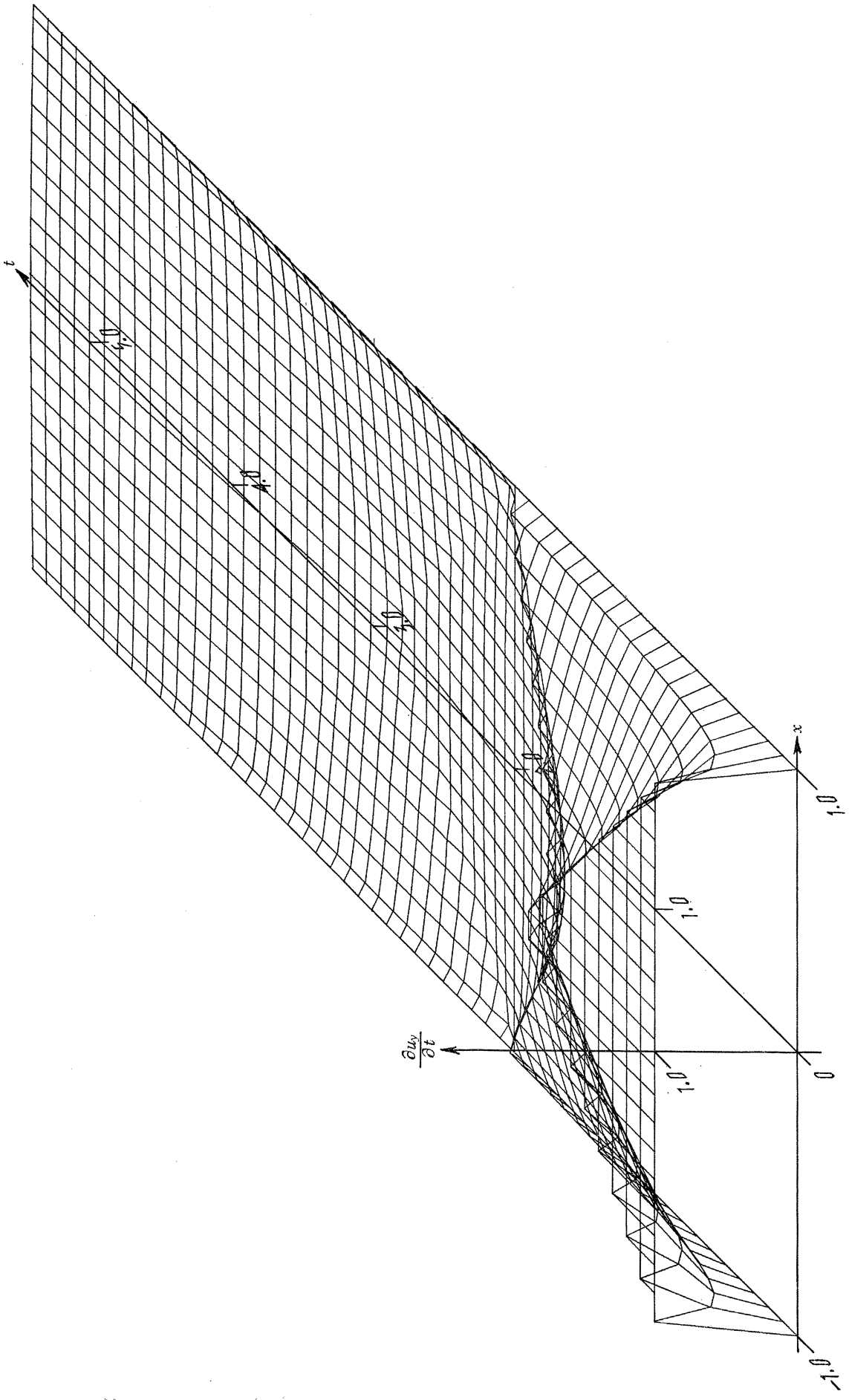

FIGURE 6. This shows the numerical solution corresponding to the analytic one shown in figure 5. We may compare the solutions as far as region D. The numerical solution is taken rather further than region D, in fact up to $t = 6$.

PHILOSOPHICAL TRANSACTIONS OF THE ROYAL SOCIETY A MATHEMATICAL, PHYSICAL & ENGINEERING SCIENCES

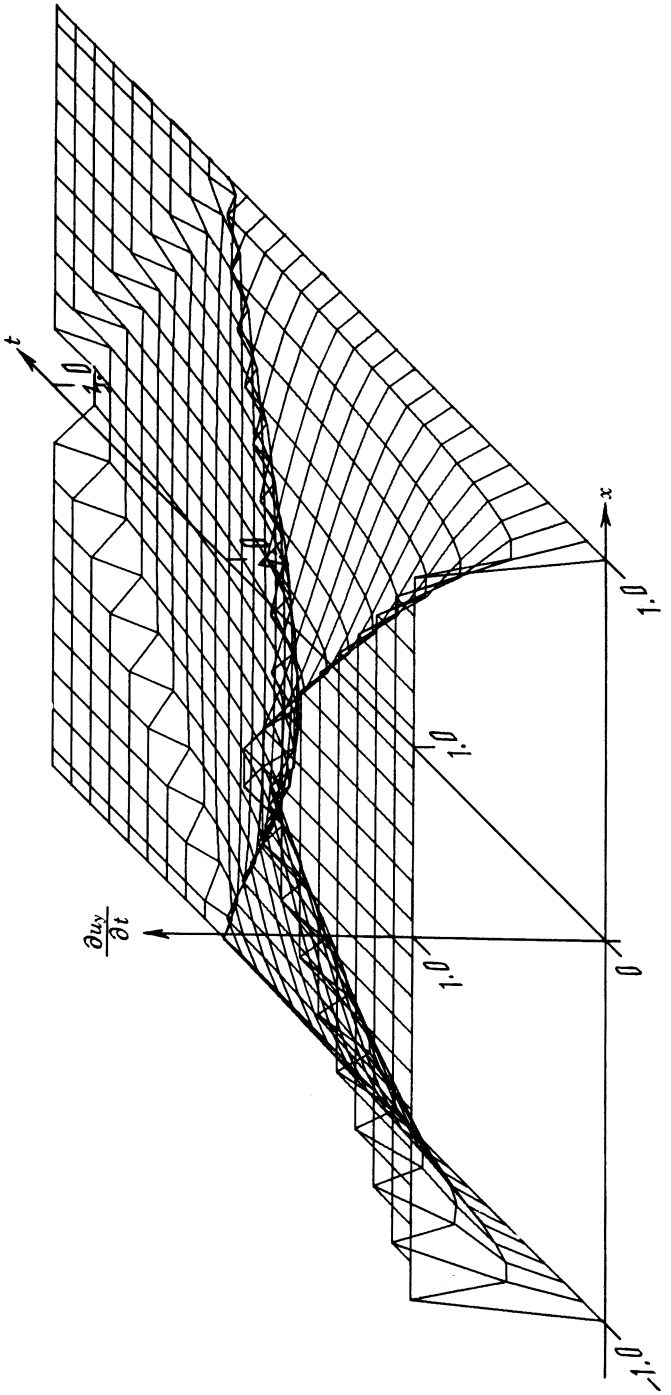

FIGURE 5. Here is shown a perspective view of the solution $\partial u_y/\partial t$ of (6.5) to (6.8) (measured vertically) for various values of t and x (measured horizontally). Beyond the region D where the solution was not computed $\partial u_y/\partial t$ was arbitrarily set to zero.

PHILOSOPHICAL TRANSACTIONS OF THE ROYAL SOCIETY A MATHEMATICAL, PHYSICAL & ENGINEERING SCIENCES

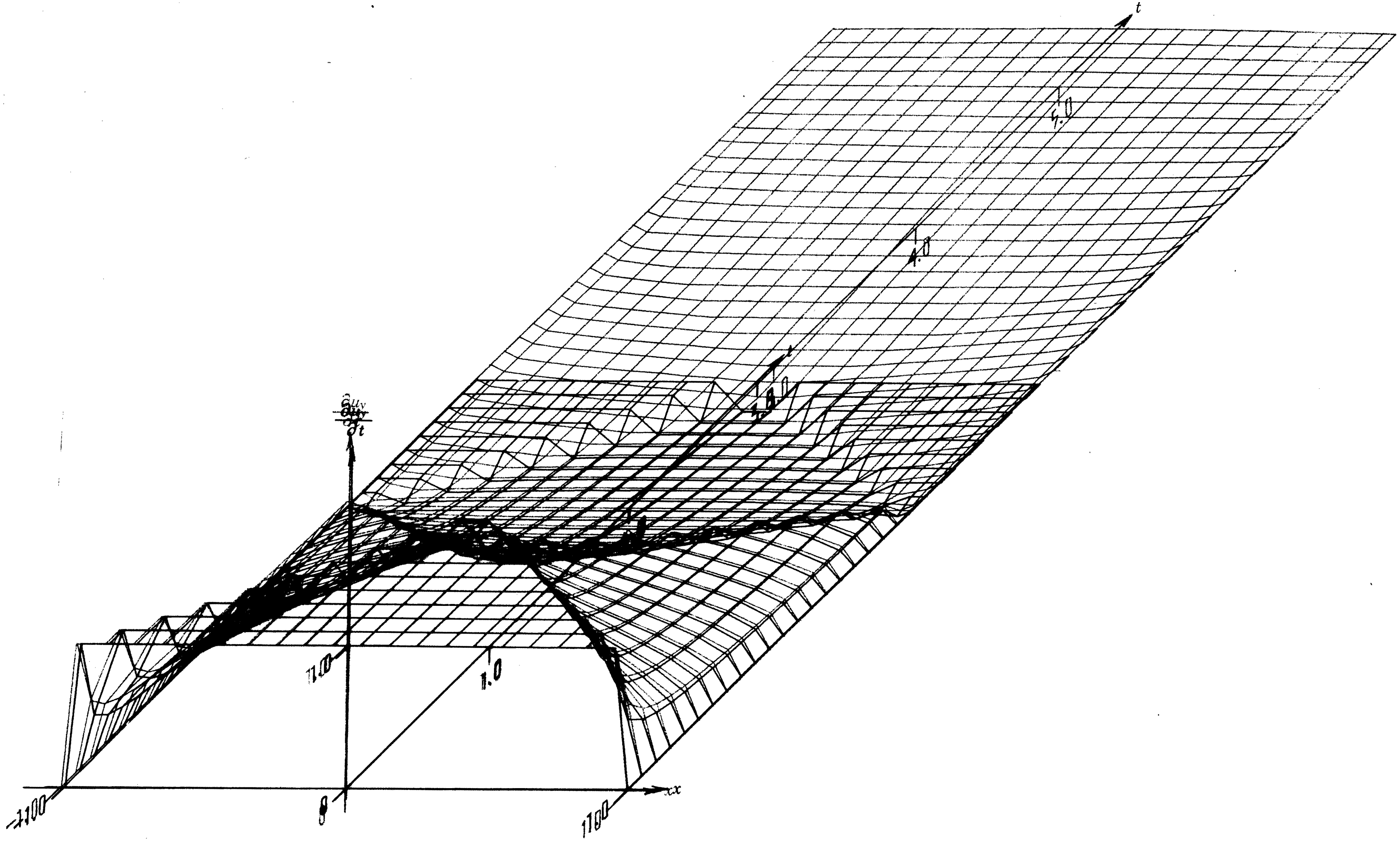

FIGURE 6. This shows the numerical solution corresponding to the analytic one shown in figure 5. We may compare the solutions as far as region D. The numerical solution is taken rather further than region D, in fact up to $t = 6$.

FIGURE 5. Here is shown a perspective view of the solution $\partial u_y/\partial t$ of (6.5) to (6.8) (measured vertically) for various values of t and x (measured horizontally). Beyond the region D where the solution was not computed $\partial u_y/\partial t$ was arbitrarily set to zero.

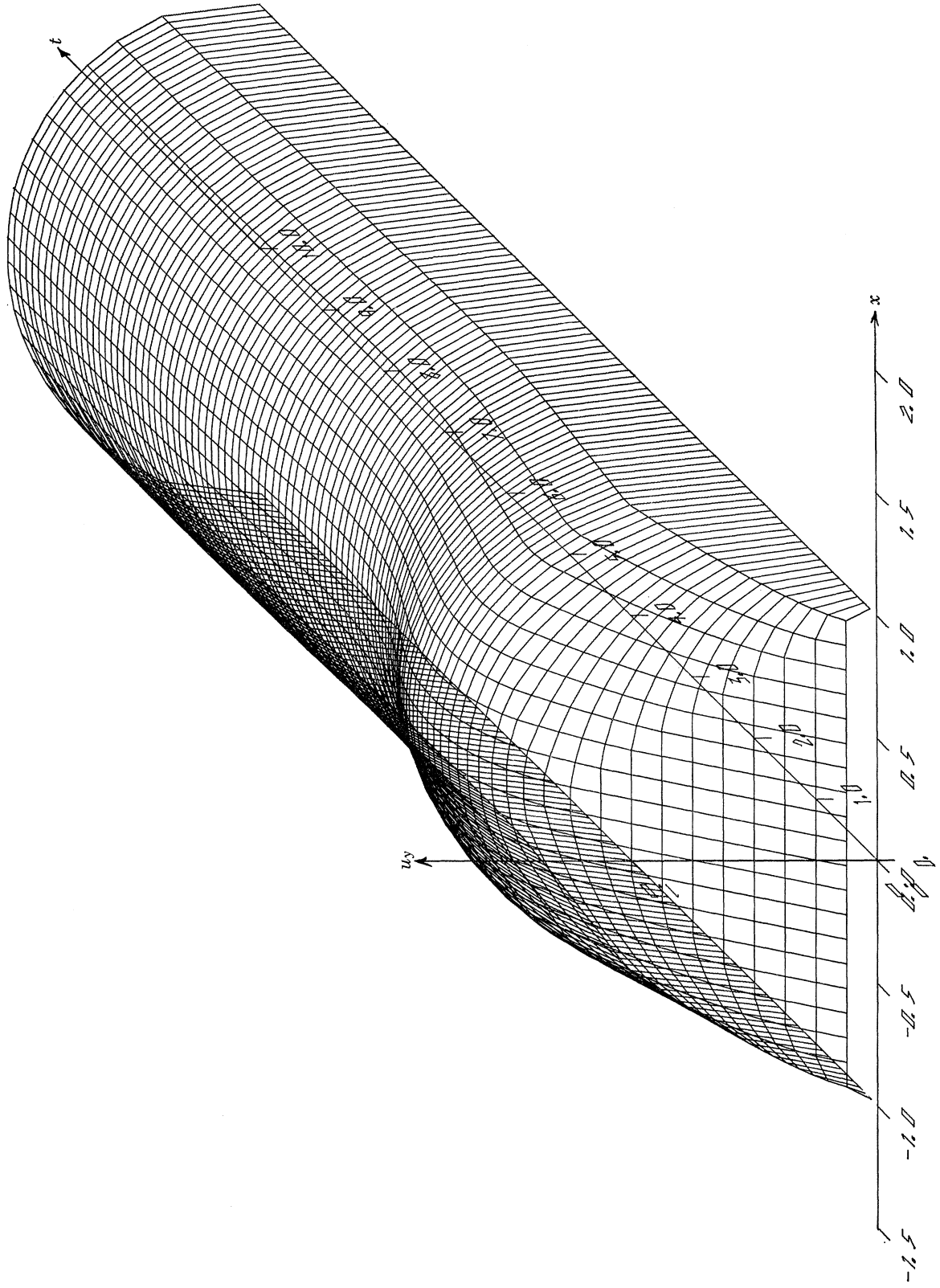

FIGURE 7. This shows the numerical solution for u_y itself taken as far as $t = 10$. By this time the solution has settled down to static values.

PHILOSOPHICAL TRANSACTIONS OF THE ROYAL SOCIETY A MATHEMATICAL, PHYSICAL & ENGINEERING SCIENCES

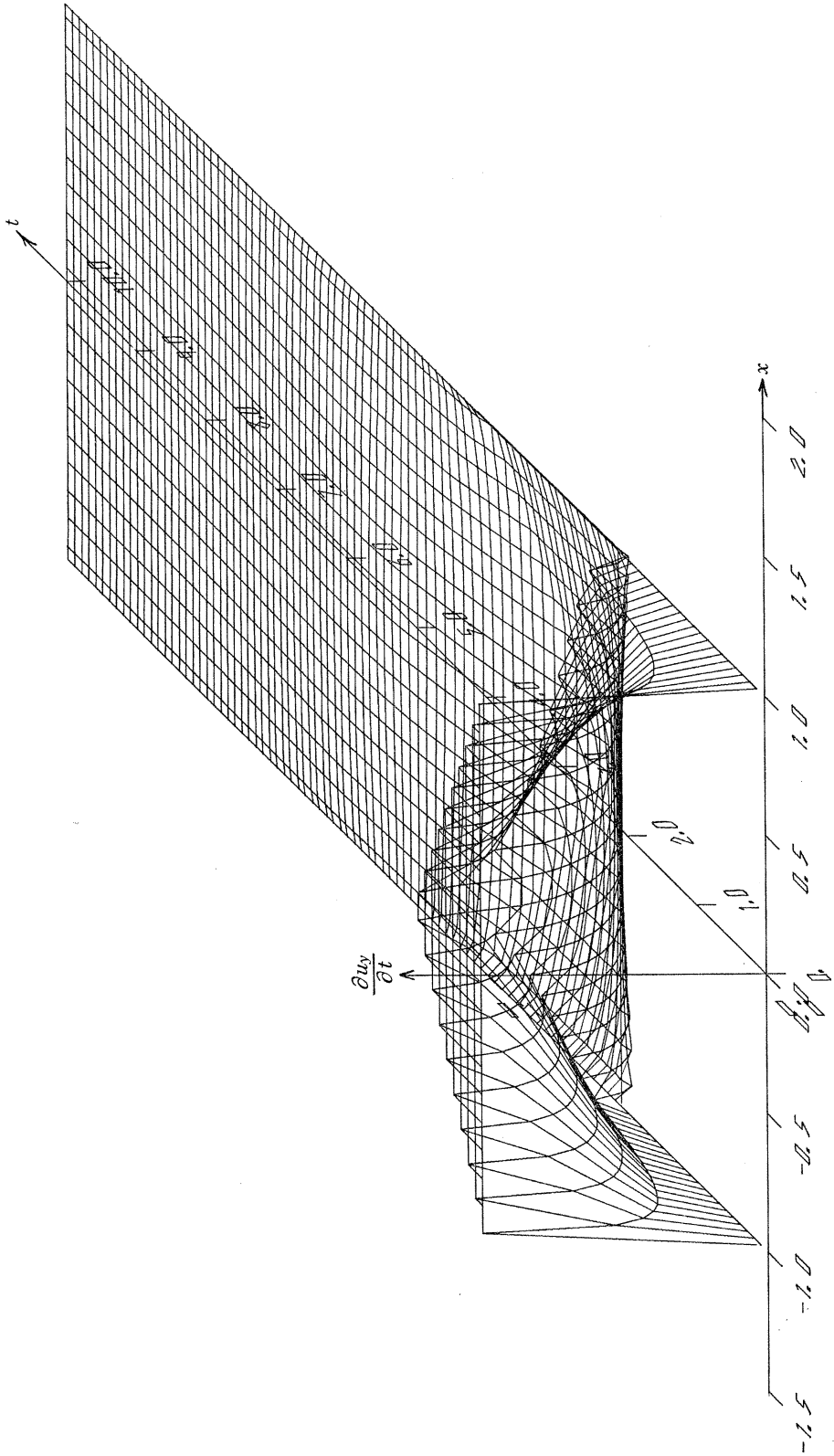

FIGURE 8. This is the time derivative $\partial u_y/\partial t$ of solution of figure 9 and the same as $\partial u_y/\partial t$ in figure 6. The enlarged vertical scale and compressed t-scale accentuates features for $t > 3$ which are missed in figure 6.

PHILOSOPHICAL TRANSACTIONS OF THE ROYAL SOCIETY A MATHEMATICAL, PHYSICAL & ENGINEERING SCIENCES

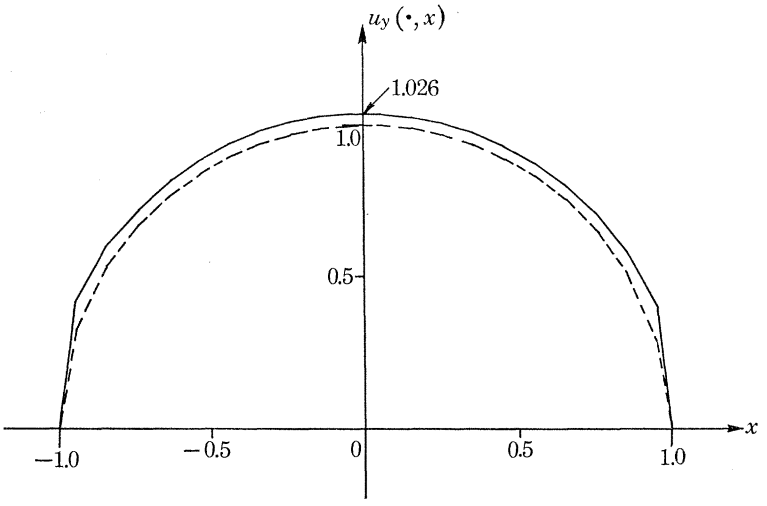

FIGURE 9. Here the numerical solution u_y of figure 7 at $t = 10$ is plotted as a function of x. The true analytic solution is plotted at the grid points. These values are joined by broken straight line segments.

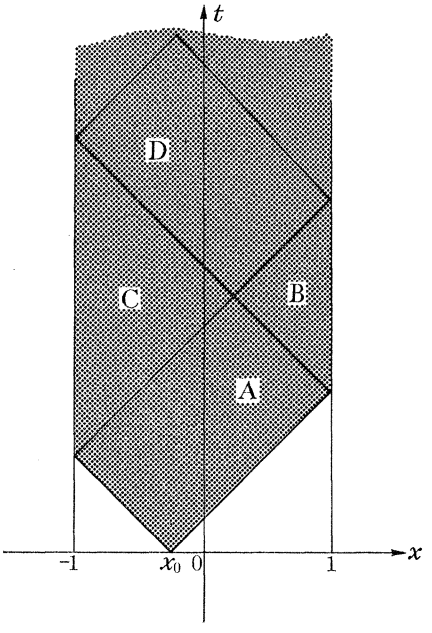

FIGURE 10. The region R hatched corresponding to the solution (6.11) to (6.14). The crack nucleates at $x = x_0$, $t = 0$ and spreads with speed 1 until it fills $-1 < x < 1$.

The region R of our next example is shown hatched in figure 10. The crack now expands from a point $x = x_0$ at $t = 0$ with unit speed in both directions until it occupies the region $-1 < x < 1$.

This also may be solved analytically quite simply by using (6.1) at least for a limited region of (t, x).

Let us change variables of integration in (6.1) to $\xi = t - x$ and $\eta = t + x$. Then (6.1) becomes

$$u_y(\xi, \eta) = \frac{1}{2\pi} \int_{\mathrm{I}} \frac{d\xi'}{(\xi - \xi')^{\frac{1}{2}}} \frac{d\eta'}{(\eta - \eta')^{\frac{1}{2}}} - \frac{1}{2\pi} \int_{\mathrm{II}} \frac{d\xi'}{(\xi - \xi')^{\frac{1}{2}}} \frac{d\eta'}{(\eta - \eta')^{\frac{1}{2}}}.$$

PHILOSOPHICAL TRANSACTIONS OF THE ROYAL SOCIETY A MATHEMATICAL, PHYSICAL & ENGINEERING SCIENCES

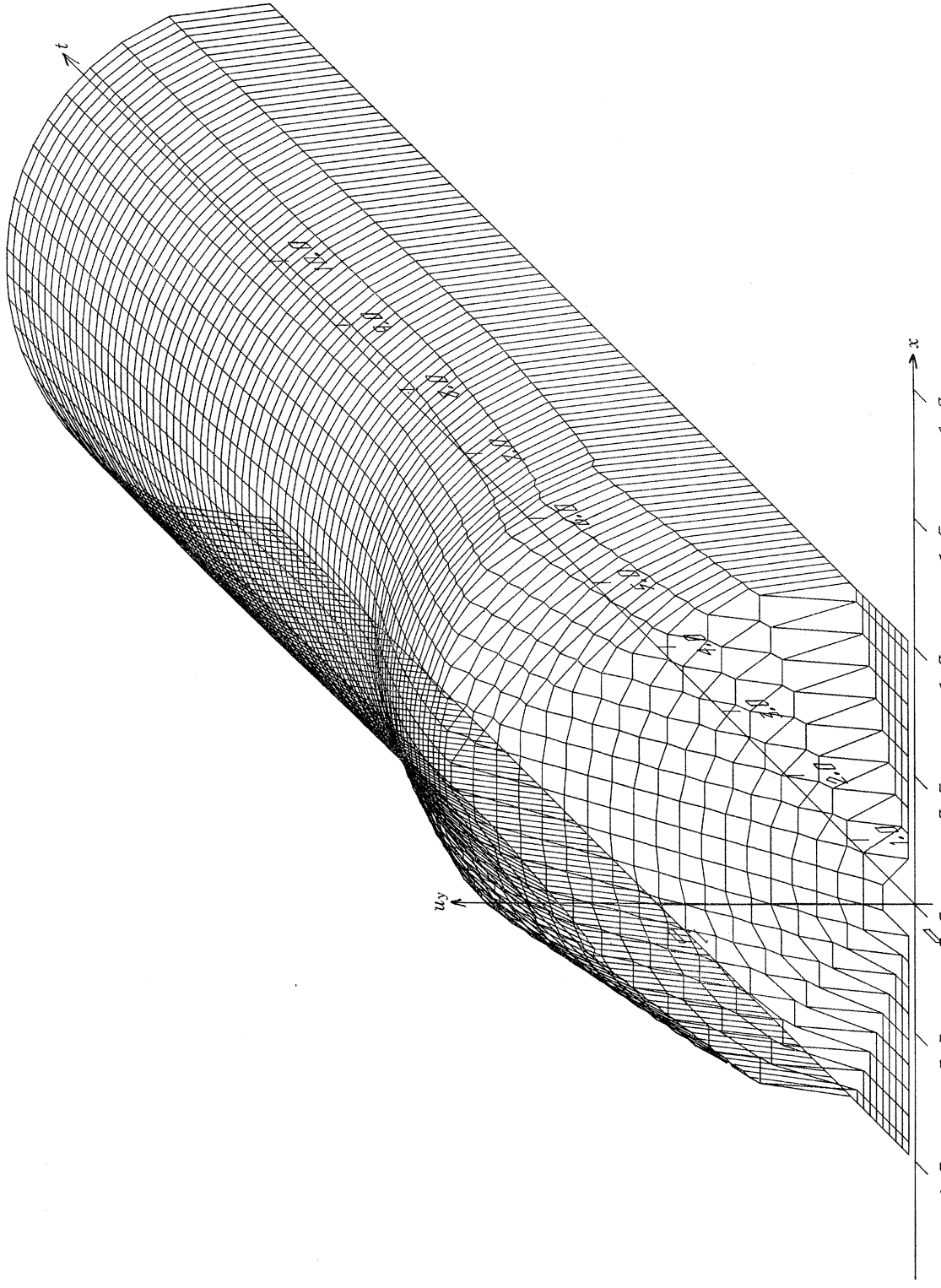

FIGURE 12. Here is shown the numerical solution corresponding to the analytic one of figure 11. It is plotted as far as $t = 10$. For (t, x) in regions A, B, C, D of figure 10 the solution shown here should be compared with that of figure 11.

PHILOSOPHICAL TRANSACTIONS OF THE ROYAL SOCIETY A MATHEMATICAL, PHYSICAL & ENGINEERING SCIENCES

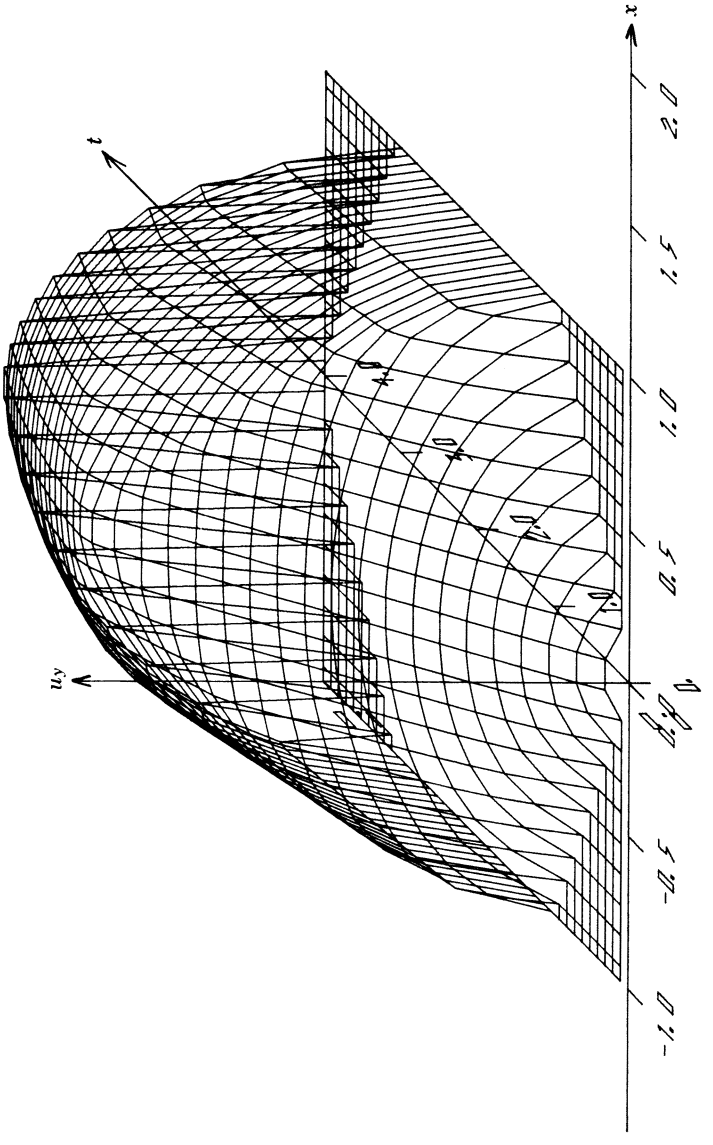

FIGURE 11. The solution of (6.11) to (6.14) is plotted as far as region D of figure 10. The value of u_y beyond region D is arbitrarily set to zero in this figure.

PHILOSOPHICAL TRANSACTIONS OF THE ROYAL SOCIETY A MATHEMATICAL, PHYSICAL & ENGINEERING SCIENCES

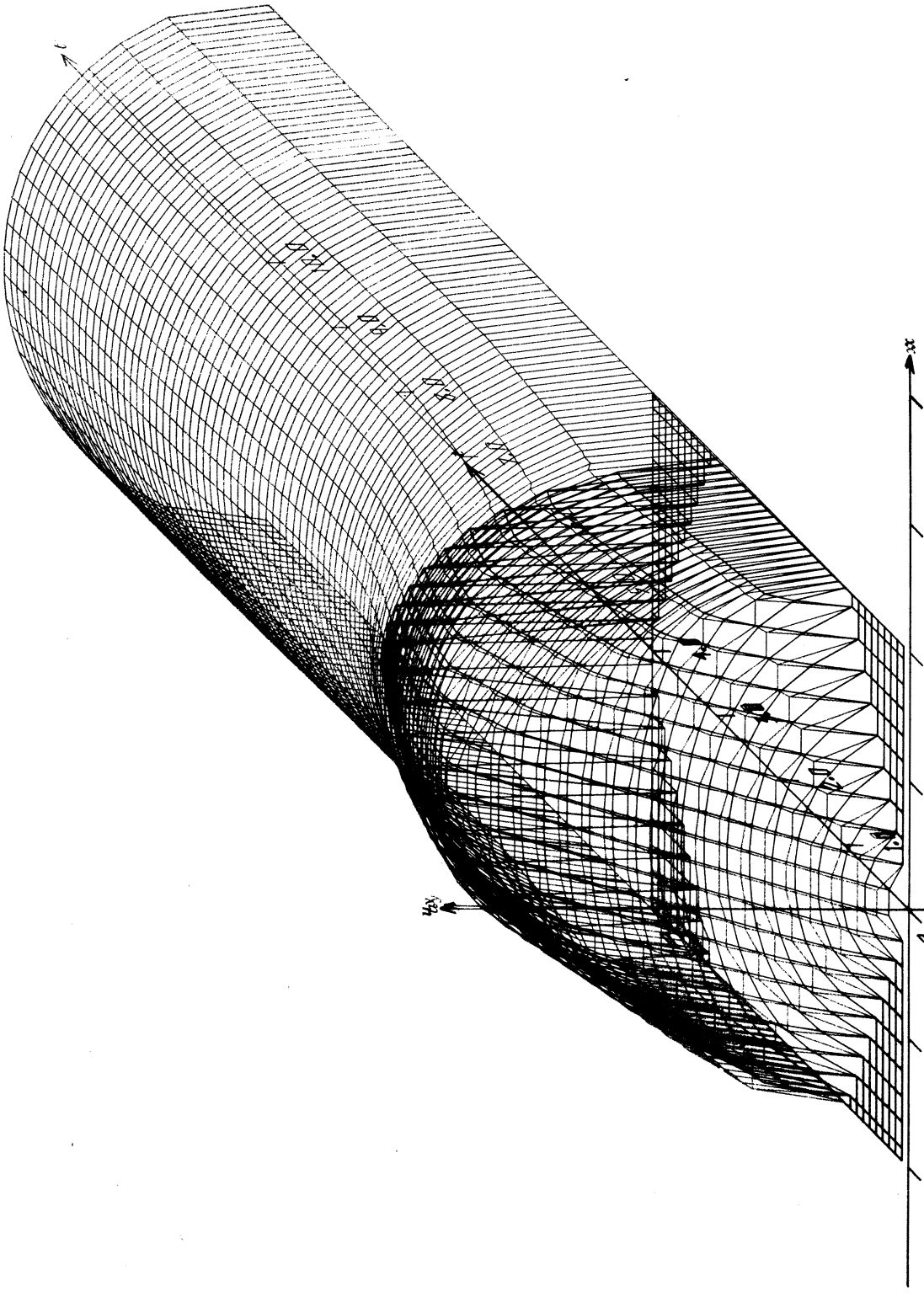

FIGURE 12. Here is shown the numerical solution corresponding to the analytic one of figure 11. It is plotted as far as $t = 10$. For (t, x) in regions A, B, C, D of figure 10 the solution shown here should be compared with that of figure 11.

FIGURE 11. The solution of (6.11) to (6.14) is plotted as far as region *D* of figure 10. The value of u_x beyond region *D* is arbitrarily set to zero in this figure.

PHILOSOPHICAL TRANSACTIONS OF THE ROYAL SOCIETY A MATHEMATICAL, PHYSICAL & ENGINEERING SCIENCES

For $(\xi, \eta) \in \mathrm{A}$

$$u_y(\xi,\eta) = \frac{1}{2\pi}\int_{-x_0}^{\xi}\frac{\mathrm{d}\xi'}{(\xi-\xi')^{\frac{1}{2}}}\int_{x_0}^{\eta}\frac{\mathrm{d}\eta'}{(\eta-\eta')^{\frac{1}{2}}}$$
$$= (1/2\pi)\times 2(\xi+x_0)^{\frac{1}{2}}\,2(\eta-x_0)^{\frac{1}{2}}$$
$$= (2/\pi)\,\{t^2-(x-x_0)^2\}^{\frac{1}{2}}. \tag{6.11}$$

For $(\xi, \eta) \in \mathrm{B}$

$$u_y(\xi,\eta) = (2/\pi)\,(\xi-\eta+2)^{\frac{1}{2}}\,(\eta-x_0)^{\frac{1}{2}}$$
$$= (2\sqrt{2}/\pi)\,(1-x)^{\frac{1}{2}}\,(t+x-x_0)^{\frac{1}{2}}. \tag{6.12}$$

For $(\xi, \eta) \in C$

$$u_y(\xi,\eta) = (2\sqrt{2}/\pi)\,(1+x)^{\frac{1}{2}}\,(t-x+x_0)^{\frac{1}{2}}. \tag{6.13}$$

For $(\xi, \eta) \in \mathrm{D}$

$$u_y(\xi,\eta) = (2\sqrt{2}/\pi)\,\{(t-x+x_0)^{\frac{1}{2}}\,(1+x)^{\frac{1}{2}}+(t+x-x_0)^{\frac{1}{2}}\,(1-x)^{\frac{1}{2}}\}-(2/\pi)\,\{t^2-(x-x_0)^2\}^{\frac{1}{2}}. \tag{6.14}$$

This solution is plotted as far as region D in figure 11 for the case when $x_0 = 0$.

The same problem solved numerically is plotted in figure 12. In the numerical work the moving boundary of the crack is specified merely by restricting the region of integration (summation) to lie within the crack area hatched in figure 10, or, what comes to the same thing, by setting $u_y = 0$ outside R.

It should be noted that in figure 11 the function plotted is arbitrarily defined to be zero for $t > 4-|x|$, that is beyond the region D.

Good agreement is obtained between the numerical and the analytic solution although the numerical solution shows some roughness mainly owing to the decoupling of the values at grid points where $i+j$ is even from those where $i+j$ is odd. Coupling is achieved after the disturbance reaches $x = \pm 1$.

7. The discretization of the kernel for plane strain

As in §§ 3 and 4 we shall set up a numerical scheme for a two-dimensional problem which is a special case of the one described in § 2. It may be specified as follows:

Let ρ, λ, μ be the density and Lamé constants of the elastic material. We shall suppose that u_y, the y component of displacement, is zero and all other quantities depend upon t, x, z only but not upon y. The region R of $z = 0$ on which the stress drops are prescribed is again a strip parallel to the y axis.

The equations to be satisfied in the half-space $z > 0$ are

$$\left.\begin{aligned}\rho\frac{\partial^2 u_x}{\partial t^2}-(\lambda+\mu)\left(\frac{\partial^2 u_x}{\partial x^2}+\frac{\partial^2 u_z}{\partial x\,\partial z}\right)-\mu\left(\frac{\partial^2 u_x}{\partial x^2}+\frac{\partial^2 u_x}{\partial z^2}\right)&=0,\\ \rho\frac{\partial^2 u_z}{\partial t^2}-(\lambda+\mu)\left(\frac{\partial^2 u_x}{\partial x\,\partial z}+\frac{\partial^2 u_z}{\partial z^2}\right)-\mu\left(\frac{\partial^2 u_z}{\partial x^2}+\frac{\partial^2 u_z}{\partial z^2}\right)&=0.\end{aligned}\right\} \tag{7.1}$$

Let us now choose units of mass and time so that $\rho = 1$ and $\lambda+2\mu = 1$. The unit of length will be chosen to be of the order of half the crack length. Equations (7.1) now simplify to

$$\left\{\begin{pmatrix}1&0\\0&1\end{pmatrix}\frac{\partial^2}{\partial t^2}-\begin{pmatrix}1&0\\0&\mu\end{pmatrix}\frac{\partial^2}{\partial x^2}-(1-\mu)\begin{pmatrix}0&1\\1&0\end{pmatrix}\frac{\partial^2}{\partial x\,\partial z}-\begin{pmatrix}\mu&0\\0&1\end{pmatrix}\frac{\partial^2}{\partial z^2}\right\}\begin{pmatrix}u_x\\u_z\end{pmatrix}=\begin{pmatrix}0\\0\end{pmatrix}. \tag{7.2}$$

The boundary conditions on $z = 0$ are given in terms of the stress drops τ_x and τ_z, and $u_x : \tau_x$ is given on R,

$$\left.\begin{aligned}u_x &= 0 \quad \text{on} \quad z=0 \quad \text{outside} \quad R,\\ \tau_z &= 0 \quad \text{on the whole of } z=0.\end{aligned}\right\} \tag{7.3}$$

PHILOSOPHICAL TRANSACTIONS OF THE ROYAL SOCIETY A MATHEMATICAL, PHYSICAL & ENGINEERING SCIENCES

But
$$\tau_x = -\mu\left(\frac{\partial u_x}{\partial z}+\frac{\partial u_z}{\partial x}\right),$$
$$\tau_z = -\lambda\left(\frac{\partial u_x}{\partial x}+\frac{\partial u_z}{\partial z}\right)-2\mu\frac{\partial u_z}{\partial z}.$$

Thus in our non-dimensionalized units

$$\left.\begin{aligned}\tau_x &= -\mu\left(\frac{\partial u_x}{\partial z}+\frac{\partial u_z}{\partial x}\right),\\ \tau_z &= -(1-2\mu)\frac{\partial u_x}{\partial x}-\frac{\partial u_z}{\partial z},\end{aligned}\right\} \tag{7.4}$$

or
$$\begin{pmatrix}\tau_x\\ \tau_z\end{pmatrix} = -\left\{\begin{pmatrix}0 & \mu\\ 1-2\mu & 0\end{pmatrix}\frac{\partial}{\partial x}+\begin{pmatrix}\mu & 0\\ 0 & 1\end{pmatrix}\frac{\partial}{\partial z}\right\}\begin{pmatrix}u_x\\ u_z\end{pmatrix}. \tag{7.5}$$

Our first task, then, is to find the kernels K_{xx}, K_{xz}, K_{zx}, and K_{zz} of § 2, but as an intermediate step let us find the kernels D_{ij} such that

$$\begin{pmatrix}D_{xx} & D_{xz}\\ D_{zx} & D_{zz}\end{pmatrix} * \begin{pmatrix}u_x\\ u_z\end{pmatrix} = -\frac{\partial}{\partial z}\begin{pmatrix}u_x\\ u_z\end{pmatrix} \tag{7.6}$$

on $z = 0$. The operation $-\partial/\partial z$ commutes with the wave operator in (7.2) so that on $z = 0$

$$\frac{\partial^2}{\partial z^2}\begin{pmatrix}u_x\\ u_z\end{pmatrix} = -\boldsymbol{D} * \frac{\partial \boldsymbol{u}}{\partial z} = \boldsymbol{D} * \boldsymbol{D} * \boldsymbol{u}. \tag{7.7}$$

Thus since u_x, u_z are arbitrary we may derive from (7.2) a quadratic equation for $\boldsymbol{D}$:

$$\begin{pmatrix}1 & 0\\ 0 & 1\end{pmatrix}\delta''(t)\,\delta(x)-\begin{pmatrix}1 & 0\\ 0 & \mu\end{pmatrix}\delta(t)\,\delta''(x)+(1-\mu)\begin{pmatrix}0 & 1\\ 1 & 0\end{pmatrix}\boldsymbol{D}*\delta(t)\,\delta'(x)-\begin{pmatrix}\mu & 0\\ 0 & 1\end{pmatrix}\boldsymbol{D}*\boldsymbol{D} = 0, \tag{7.8}$$

which is the analogue of (4.5). Once the δ functions have been replaced by suitable discretizations $\boldsymbol{D}$ is computed numerically by a method which closely parallels that of section 4 ((4.6) *et seq.*).

Again we choose the time step equal to the space step (call it h) and then discretize $\delta''(t)\,\delta(x)$ and $\delta(t)\,\delta''(x)$ as before, and $\delta(t)\,\delta'(x)$ as in table 4. Consideration of domains of dependence leads us to the fact that each component $D_{xx}, D_{xz}, D_{zx}, D_{zz}$ of $\boldsymbol{D}$ is a triangular array, zero except for $|j| \leqslant i$.

TABLE 4. THE DISCRETIZATION OF $\delta(t)\,\delta'(x)$

i \ j	-1	0	1
0	0	0	0
1	$1/2h$	0	$-1/2h$
2	0	0	0

If $\boldsymbol{D}(i,j)$ is known in all components up to $i = i_0 - 1$, then if we write (7.8) for $j = j_0$, $i = i_0$ the only terms involving $\boldsymbol{D}(i_0,j_0)$ arise in $\boldsymbol{D} * \boldsymbol{D}$ and are transferred to the other side of the equation. When this is done we have an equation for the $D_{pq}(i_0,j_0)$ in terms of the $D_{pq}\,(i,j)$ with $i < i_0\,(p,q = x,z)$. Thus $\boldsymbol{D}$ may be computed recursively.

Let us write $\boldsymbol{D}(i,j) = 1/h\,\bar{\boldsymbol{D}}(i,j)$. Then for $\mu = \frac{1}{3}$ (Poisson solid) the first few values of $\bar{\boldsymbol{D}}$ are as in tables 5 to 8.

Having computed $\boldsymbol{D}$ we may rewrite (7.5) as

$$\begin{pmatrix}\tau_{zx}\\ \tau_{xz}\end{pmatrix} = \left\{-\begin{pmatrix}0 & \mu\\ 1-2\mu & 0\end{pmatrix}\delta(t)\,\delta'(x) + \begin{pmatrix}\mu & 0\\ 0 & 1\end{pmatrix}\boldsymbol{D}\right\} * \begin{pmatrix}u_x\\ u_z\end{pmatrix}. \tag{7.9}$$

Thus
$$\begin{pmatrix}K_{xx} & K_{xz}\\ K_{zx} & K_{zz}\end{pmatrix} = \begin{pmatrix}\mu D_{xx} & \mu(D_{xz} - \delta(t)\,\delta'(x))\\ D_{zx} - (1-2\mu)\,\delta(t)\,\delta'(x) & D_{zz}\end{pmatrix}, \tag{7.10}$$

where $\delta(t)\,\delta'(x)$ is discretized as in table 4 and $\bar{\boldsymbol{D}} = 1/h\boldsymbol{D}$ with $\bar{\boldsymbol{D}}$ given in tables 5 to 8.

For $\mu = \frac{1}{3}$ the first few values of $\bar{\boldsymbol{K}}$ are as in tables 9 to 12, where $\boldsymbol{K} = (1/h)\,\bar{\boldsymbol{K}}$.

TABLE 5. THE ARRAY $\bar{D}_{xx}(i,j)$

i \ j	−5	−4	−3	−2	−1	0	1	2	3	4	5
0	0.000000	0.000000	0.000000	0.000000	0.000000	1.732051	0.000000	0.000000	0.000000	0.000000	0.000000
1	0.000000	0.000000	0.000000	0.000000	−0.866025	0.000000	−0.866025	0.000000	0.000000	0.000000	0.000000
2	0.000000	0.000000	0.000000	−0.177831	0.000000	0.355662	0.000000	−0.177831	0.000000	0.000000	0.000000
3	0.000000	0.000000	−0.098353	0.018875	0.098353	−0.037750	0.098353	0.018875	−0.098353	0·000000	0.000000
4	0.000000	−0.064443	0.015112	0.049716	−0.015112	0.029453	−0.015112	0.049716	0.015112	−0.064443	0.000000
5	−0.046538	0.010254	0.037978	−0.015578	0·008559	0.010649	0·008559	−0.015578	0.037978	0.010254	−0.046538

TABLE 6. THE ARRAY $\bar{D}_{xz}(i,j)$

i \ j	−5	−4	−3	−2	−1	0	1	2	3	4	5
0	0.000000	0.000000	0.000000	0.000000	0.000000	0.000000	0.000000	0.000000	0.000000	0.000000	0.000000
1	0.000000	0.000000	0.000000	0.000000	0.366025	0.000000	−0.366025	0.000000	0.000000	0.000000	0.000000
2	0.000000	0.000000	0.000000	0.077350	−0.154701	0.000000	0.154701	−0.077350	0.000000	0.000000	0.000000
3	0.000000	0.000000	0.055021	−0.065384	−0.034295	0.000000	0.034295	0.065384	−0.055021	0.000000	0.000000
4	0.000000	0.041287	−0.027635	−0.070276	0.058310	0.000000	−0.058310	0.070276	0.027635	−0.041287	0.000000
5	0.032329	−0.010912	−0.063223	0.024836	0.022001	0.000000	−0.022001	−0.024836	0.063223	0.010912	−0.032329

TABLE 7. THE ARRAY $\bar{D}_{zx}(i,j)$

i \ j	−5	−4	−3	−2	−1	0	1	2	3	4	5
0	0.000000	0.000000	0.000000	0.000000	0.000000	0.000000	0.000000	0.000000	0.000000	0.000000	0.000000
1	0.000000	0.000000	0.000000	0.000000	0.211325	0.000000	−0.211325	0.000000	0.000000	0.000000	0.000000
2	0.000000	0.000000	0.000000	−0.025783	0.051567	0.000000	−0.051567	0.025783	0.000000	0.000000	0.000000
3	0.000000	0.000000	−0.018340	0.021795	0.011432	0.000000	−0.011432	−0.021795	0.018340	0.000000	0.000000
4	0.000000	−0.013762	0.009212	0.023425	−0.019437	0.000000	0.019437	−0.023425	−0.009212	0.013762	0.000000
5	−0.010776	0.003637	0.021074	−0.008279	−0.007334	0.000000	0.007334	0.008279	−0.021074	−0.003637	0.010776

TABLE 8. THE ARRAY $\bar{D}_{zz}(i,j)$

i \ j	−5	−4	−3	−2	−1	0	1	2	3	4	5
0	0.000000	0.000000	0.000000	0.000000	0.000000	1.000000	0.000000	0.000000	0.000000	0.000000	0.000000
1	0.000000	0.000000	0.000000	0.000000	−0.166667	−0.666667	−0.166667	0.000000	0.000000	0.000000	0.000000
2	0.000000	0.000000	0.000000	0.008440	−0.111111	0.205342	−0.111111	0.008440	0.000000	0.000000	0.000000
3	0.000000	0.000000	0.010844	−0.031766	−0.047881	0.137607	−0.047881	−0.031766	0.010844	0.000000	0.000000
4	0.000000	0.009482	−0.009093	−0.042165	0.021439	0.040675	0.021439	−0.042165	−0.009093	0.009482	0.000000
5	0.007945	−0.001616	−0.027986	−0.009714	0.040617	−0.018492	0.040617	−0.009714	−0.027986	−0.001616	0.007945

PHILOSOPHICAL TRANSACTIONS OF THE ROYAL SOCIETY A MATHEMATICAL, PHYSICAL & ENGINEERING SCIENCES

TABLE 9. THE ARRAY $\bar{K}_{xx}(i,j)$

i \ j	−5	−4	−3	−2	−1	0	1	2	3	4	5
0	0.000000	0.000000	0.000000	0.000000	0.000000	0.577350	0.000000	0·000000	0.000000	0.000000	0.000000
1	0.000000	0.000000	0.000000	0.000000	−0.288675	0.000000	−0.288675	0.000000	0.000000	0.000000	0.000000
2	0.000000	0.000000	0.000000	−0.059277	0.000000	0.118554	0.000000	−0.059227	0.000000	0.000000	0.000000
3	0.000000	0.000000	−0.032784	0.006292	0.032784	−0.012583	0.032784	0.006292	−0.032784	0.000000	0.000000
4	0.000000	−0.021481	0.005037	0.016572	−0.005037	0.009818	−0.005037	0.016572	0.005037	−0.021481	0.000000
5	−0.015513	0.003418	0.012659	−0.005193	0.002853	0.003550	0.002853	−0.005193	0.012659	0.003418	−0.015513

TABLE 10. THE ARRAY $\bar{K}_{xz}(i,j)$

i \ j	−5	−4	−3	−2	−1	0	1	2	3	4	5
0	0.000000	0.000000	0.000000	0.000000	0.000000	0.000000	0.000000	0.000000	0.000000	0.000000	0.000000
1	0.000000	0.000000	0.000000	0.000000	−0.044658	0.000000	0.044658	0.000000	0.000000	0.000000	0.000000
2	0.000000	0.000000	0.000000	0.025783	−0.051567	0.000000	0.051567	−0.025783	0.000000	0.000000	0.000000
3	0.000000	0.000000	0.018340	−0.021795	−0.011432	0.000000	0.011432	0.021795	−0.018340	0.000000	0.000000
4	0.000000	0.013762	−0.009212	−0.023425	0.019437	0.000000	−0.019437	0.023425	0.009212	−0.013762	0.000000
5	0.010776	−0.003637	−0.021074	0.008279	0.007334	0.000000	−0.007334	−0.008279	0.021074	0.003637	−0.010776

TABLE 11. THE ARRAY $\bar{K}_{zx}(i,j)$

i \ j	−5	−4	−3	−2	−1	0	1	2	3	4	5
0	0.000000	0.000000	0.000000	0.000000	0.000000	0.000000	0.000000	0.000000	0.000000	0.000000	0.000000
1	0.000000	0.000000	0.000000	0.000000	0.044658	0.000000	−0.044658	0.000000	0.000000	0.000000	0.000000
2	0.000000	0.000000	0.000000	−0.025783	0.051567	0.000000	−0.051567	0.025783	0.000000	0.000000	0.000000
3	0.000000	0.000000	−0.018340	0.021795	0.011432	0.000000	−0.011432	−0.021795	0.018340	0.000000	0.000000
4	0.000000	−0.013762	0.009212	0.023425	−0.019437	0.000000	0.019437	−0.023425	−0.009212	0.013762	0.000000
5	−0.010776	0.003637	0.021074	−0.008279	−0.007334	0.000000	0.007334	0.008279	−0.021074	−0.003637	0.010776

TABLE 12. THE ARRAY $\bar{K}_{zz}(i,j)$

i \ j	−5	−4	−3	−2	−1	0	1	2	3	4	5
0	0.000000	0.000000	0.000000	0.000000	0.000000	1.000000	0.000000	0.000000	0.000000	0.000000	0.000000
1	0.000000	0.000000	0.000000	0.000000	−0.166667	−0.666667	−0.166667	0.000000	0.000000	0.000000	0.000000
2	0.000000	0.000000	0.000000	0.008440	−0.111111	0.205342	−0.111111	0.008440	0.000000	0.000000	0.000000
3	0.000000	0.000000	0.010844	−0.031766	−0.047881	0.137607	−0.047881	−0.031766	0.010844	0.000000	0.000000
4	0.000000	0.009482	−0.009093	−0.042165	0.021439	0.040675	0.021439	−0.042165	−0.009093	0.009482	0.000000
5	0.007945	−0.001616	−0.027986	−0.009714	0.040617	−0.018492	0.040617	−0.009714	−0.027986	−0.001616	0.007945

8. SOME NUMERICAL RESULTS FOR PLANE STRAIN

It is now straightforward to set up equations (2.9) and (2.10) for plane strain. The equations become

$$\tau_x(t,x) = \int_{C\cap R} K_{xx}(t-t', x-x')\, u_x(t',x')\, \mathrm{d}t'\, \mathrm{d}x' + \int_C K_{xz}(t-t', x-x') u_z(t',x')\, \mathrm{d}t'\, \mathrm{d}x', \tag{8.1}$$

$$0 = \int_{C\cap R} K_{zx}(t-t', x-x')\, u_x(t',x')\, \mathrm{d}t'\, \mathrm{d}x' + \int_C K_{zz}(t-t', x-x')\, u_z(t',x')\, \mathrm{d}t'\, \mathrm{d}x'. \tag{8.2}$$

PHILOSOPHICAL TRANSACTIONS OF THE ROYAL SOCIETY A MATHEMATICAL, PHYSICAL & ENGINEERING SCIENCES

The numerical method is a direct extension of (5.2), (5.3):

$$\bar{K}_{xx}(0,0)\,u_x(i_0,j_0) = h\tau_x(i_0,j_0) - \sum_{i<i_0}\sum \bar{K}_{xx}(i_0-i, j_0-j)\,u_x(i,j) - \sum_{i<i_0}\sum \bar{K}_{xz}(i_0-i, j_0-j)\,u_z(i,j), \quad (8.3)$$

$$\bar{K}_{zz}(0,0)\,u_z(i_0,j_0) = -\sum_{i<i_0}\sum \bar{K}_{zx}(i_0-i, j_0-j)\,u_x(i,j) - \sum_{i<i_0}\sum \bar{K}_{zz}(i_0-i, j_0-j)\,u_z(i,j). \quad (8.4)$$

In the first sums in (8.3) and (8.4) the summation is restricted to the region R of the crack since $u_x(i,j) = 0$ outside R. However, the summations in the second sums are not so restricted. The normal displacement u_z, which represents the warping of the fault plane, is non-zero even outside R. Thus in (8.4) we consider values of (i_0,j_0) outside R also. The figures which follow represent some solutions for constant stress drop τ_x and different forms for the region R.

Figures 13 and 14 show the numerical solutions when $\tau_x = 1$ and $R(t)$ instantaneously attains its maximum size at $t = 0$ and thereafter occupies the same region $-1 < x < 1$ for all time. The solution was carried out with eight discretization steps across the crack and forty in the time direction. Notice that the solution overshoots the static solution, u_x attaining a maximum of 2.738 (for $x = \pm 0.125$) at about $t = 3$ after which it decreases and has essentially reached the static solution by $t = 9$ or 10.

After attaining its maximum the tangential displacement u_x does not oscillate but decreases monotonically to its static value (2.333 at $x = \pm 0.125$). In this respect the motion contrasts with that for antiplane strain where the solution continues to oscillate with heavily damped oscillations.

The normal displacement u_z is shown in figure 14. We see clearly a rather smooth S-wave propagating in the $\pm x$ directions, especially for $t > 5$.

Here u_z attains its maximum of 0.884 at $x = 0.875$ and like u_x it then decreases monotonically to a static value by about $t = 9$ in the region of the crack, that is for $-1.5 < x < 1.5$, say. Away from the crack we cannot expect the static solution to be attained at all points since the waves produced by the crack are still travelling. They are still evident in the diagram when the solution is terminated at $t = 10$.

The values of u_x and u_z at $t = 10$ may be compared with the values obtained for the corresponding static problem by Starr (1928). His formula (16), after the addition of a rigid rotation

$$u_x = -\tfrac{3}{4}z, \quad u_z = \tfrac{3}{4}x$$

to bring the displacement to zero at infinity, gives on $z = 0$

$$\left.\begin{aligned} u_x &= \tfrac{9}{4}(1-x^2)^{\frac{1}{2}} \quad \text{for} \quad -1 < x < 1,\\ &= 0 \quad \text{for} \quad |x| > 1;\\ u_z &= \tfrac{3}{4}(x+(x^2-1)^{\frac{1}{2}}) \quad \text{for} \quad x < -1,\\ &= \tfrac{3}{4}x \quad \text{for} \quad -1 < x < 1,\\ &= \tfrac{3}{4}(x-(x^2-1)^{\frac{1}{2}}) \quad \text{for} \quad 1 < x. \end{aligned}\right\} \quad (8.5)$$

Figure 15 shows these functions plotted together with our numerical solutions for $t = 10$. Agreement is obtained to within 4 % at the centre of the crack which is less than the uncertainty in the position of the boundary owing to the coarseness of the discretion.

Figures 16 and 17 show the tangential and normal displacements due to a crack which is nucleated at the origin at $t = 0$ and then spreads out at half the P-wave speed (that is 0.5 in our non-dimensional units) in both directions until it occupies the region $-1 < x < 1$ after

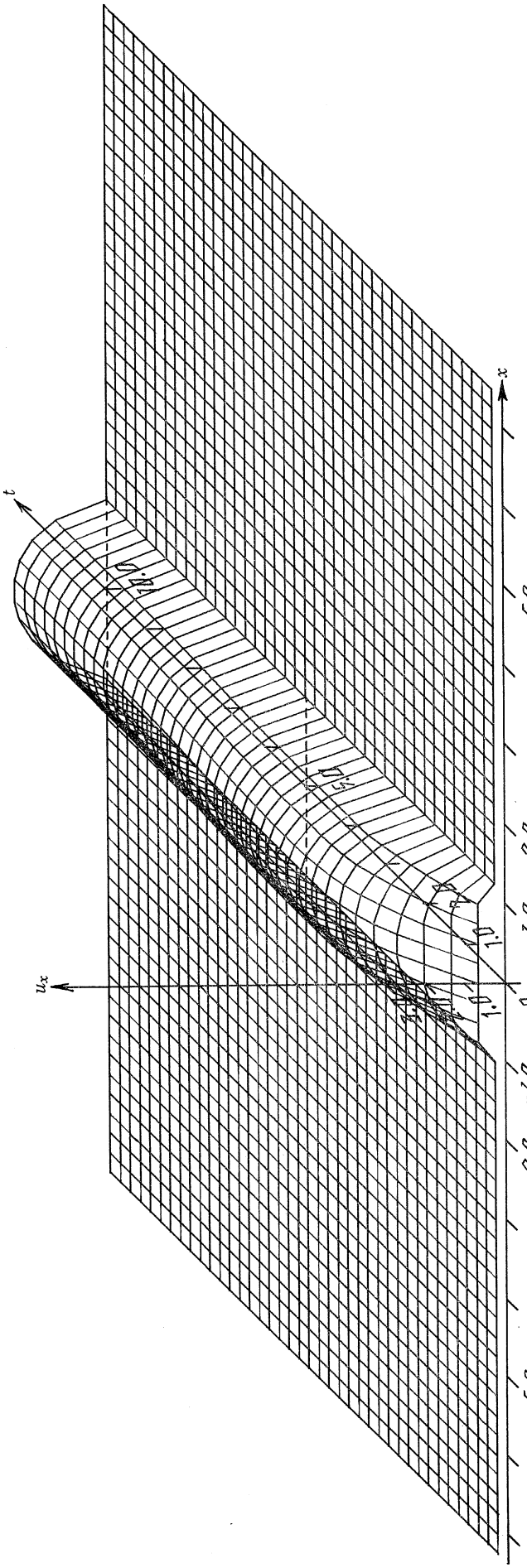

FIGURE 13. This shows the tangential component of displacement u_x plotted as far as $t = 10$ for a crack which instantaneously attains its maximum width at $t = 0$. The solution overshoots the static value to which it returns asymptotically.

PHILOSOPHICAL TRANSACTIONS OF THE ROYAL SOCIETY A MATHEMATICAL, PHYSICAL & ENGINEERING SCIENCES

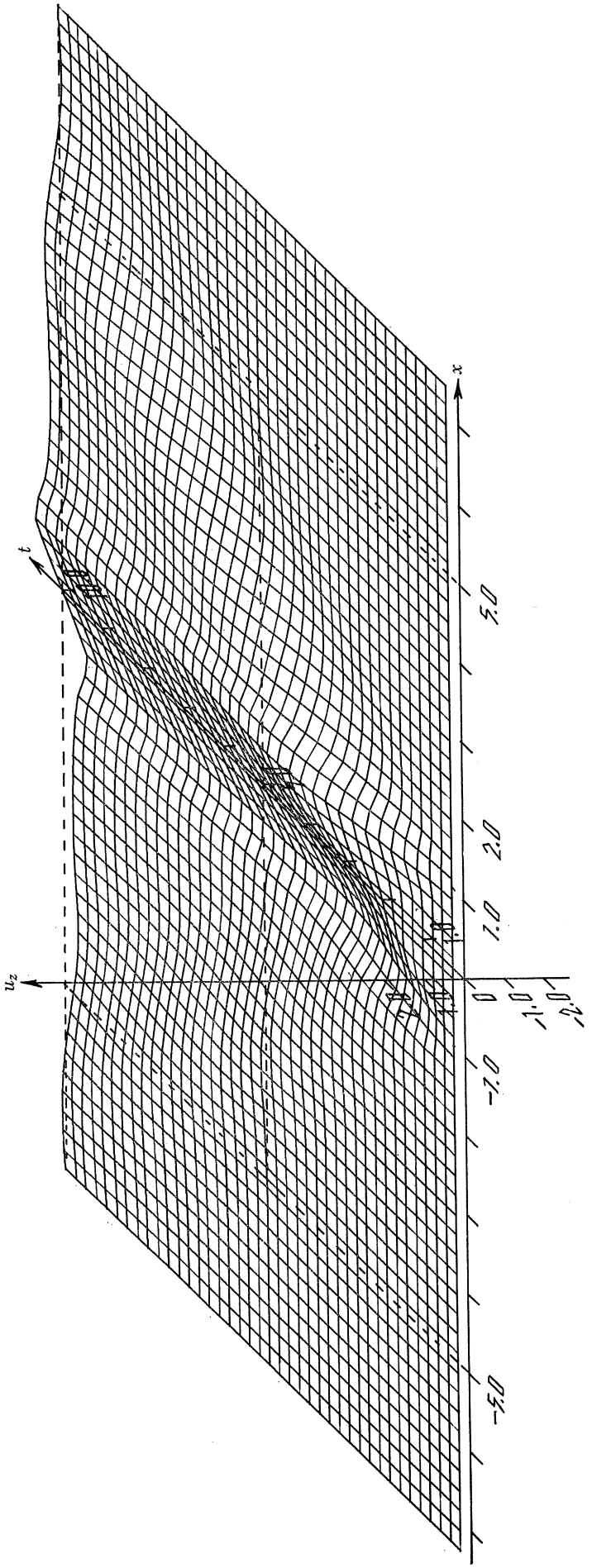

FIGURE 14. Here is shown the normal component of displacement u_z on $z = 0$. Notice this is non-zero even beyond the crack tips $x = \pm 1$. An S wave is clearly seen travelling away from the crack.

PHILOSOPHICAL TRANSACTIONS OF THE ROYAL SOCIETY A MATHEMATICAL, PHYSICAL & ENGINEERING SCIENCES

which it spreads no further. The ripples on the solution are due to the discretization of the moving edges of the crack and these rapidly die out when the crack stops spreading. Notice that the tangential displacement continues to increase even after the crack has reached its maximum size and overshoots its static value like the u_x shown in figure 11. If we were to consider this solution as a model of a seismic source it is most likely that the slipping would cease when u_x attained its maximum value since friction would then oppose the tendency for u_x to return to its static value.

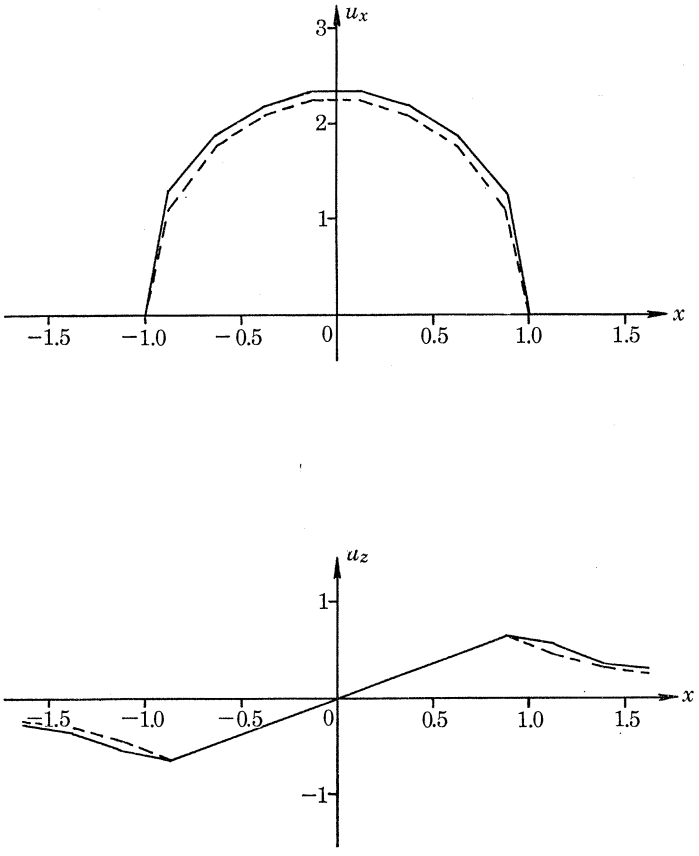

FIGURE 15. Here we may compare the values of u_x and u_z obtained numerically for $t = 10$ (full lines) with the analytic solution of the corresponding static problem (broken lines).

In figures 18 and 19 are shown the solutions u_x and u_z with more resolution when $\tau_x(t, x) = \delta(t)$ on the crack $-1 < x < 1$. In 18 the two P waves diffracted from the edges are very clear. Smooth diffracted S waves are also evident. In figure 19 the corresponding diffracted P is smooth but the S is rather more distinct. These differences in the appearances of the diffracted P and S waves crossing the crack in figures 18 and 19 are due mainly to the differences in polarization of the two types of waves.

Notice also in figure 19 the S wave propagating beyond the edges of the crack. The P propagating in this region is not evident in agreement with its direction of polarization.

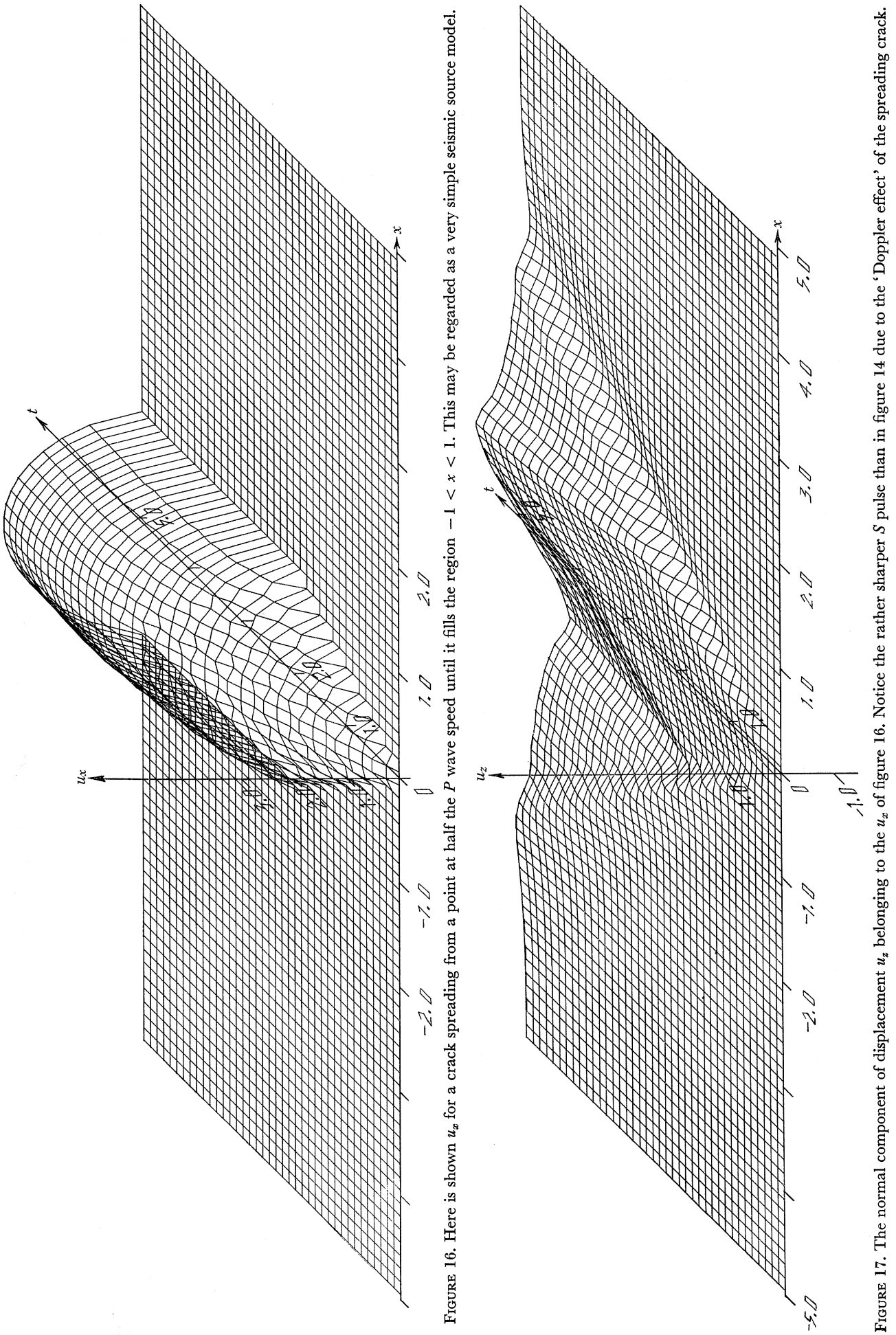

FIGURE 16. Here is shown u_x for a crack spreading from a point at half the P wave speed until it fills the region $-1 < x < 1$. This may be regarded as a very simple seismic source model.

FIGURE 17. The normal component of displacement u_z belonging to the u_x of figure 16. Notice the rather sharper S pulse than in figure 14 due to the 'Doppler effect' of the spreading crack.

PHILOSOPHICAL TRANSACTIONS OF THE ROYAL SOCIETY A MATHEMATICAL, PHYSICAL & ENGINEERING SCIENCES

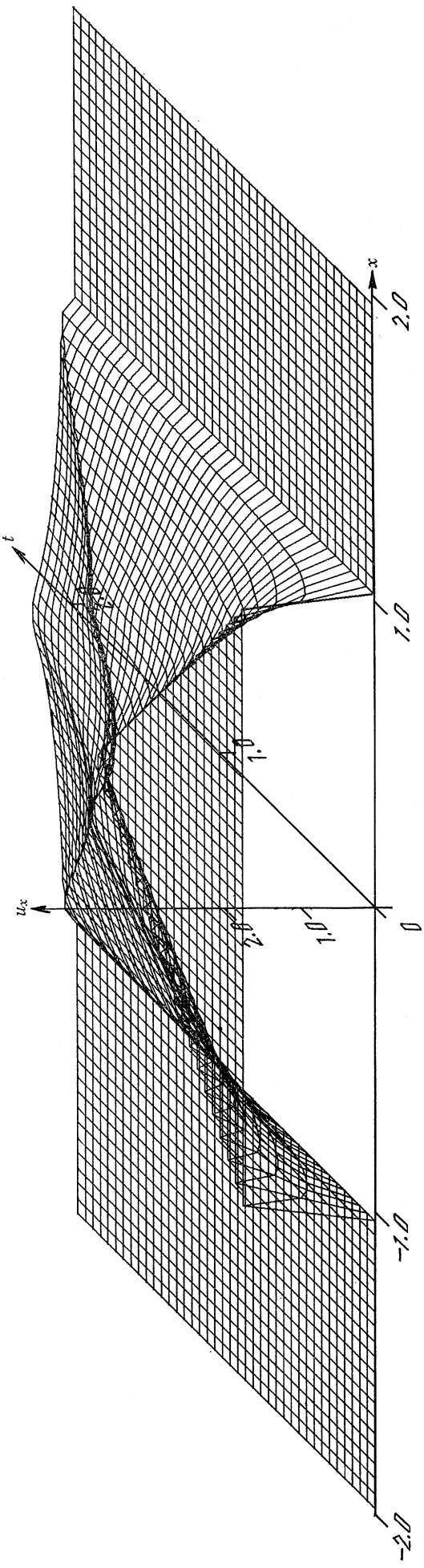

FIGURE 18. Here is shown the tangential displacement u_x corresponding to a normally incident S wave with $\delta(t)$ time dependence on a crack of half-width unity. Diffracted P and S waves are clear.

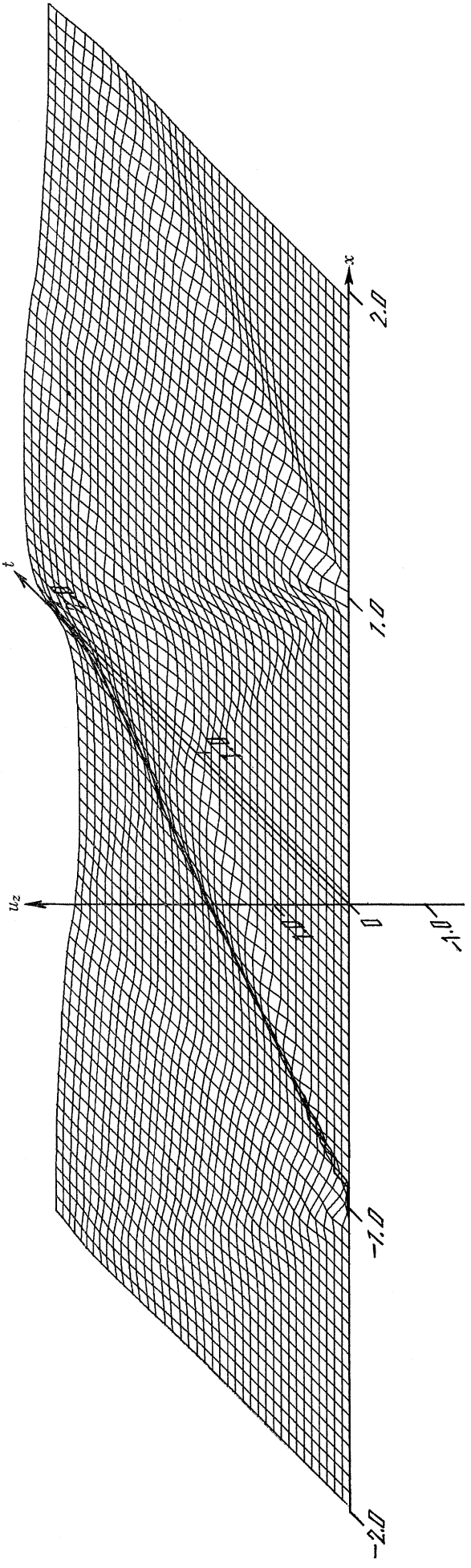

FIGURE 19. The normal displacement u_z corresponding to the u_x of figure 18. Notice the clear P and S waves diffracted from the edges $x = \pm 1$ of the crack.

PHILOSOPHICAL TRANSACTIONS OF THE ROYAL SOCIETY A MATHEMATICAL, PHYSICAL & ENGINEERING SCIENCES

9. Elimination of the normal displacement

Since the values of the displacement discontinuity across $z = 0$ determine the displacements everywhere (see, for instance, Burridge & Knopoff 1964) the determination of u_z is redundant in so far as we wish eventually to calculate the radiation out of the plane of the crack. We now show more explicitly how u_z may be eliminated following the scheme of (2.11) to (2.16).

We solve (8.2) for u_z:

$$u_z = -K_{zz}^{-1} * K_{zx} * u_x, \tag{9.1}$$

where K_{zz}^{-1} is defined by

$$K_{zz} * K_{zz}^{-1} = \delta(t)\,\delta(x). \tag{9.2}$$

Substituting this value of u_z in (8.1) we obtain

$$(K_{xx} - K_{zz}^{-1} * K_{zx} * K_{xz}) * u_x = \tau_x. \tag{9.3}$$

Thus we need to compute the new kernel

$$L \equiv K_{xx} - K_{zz}^{-1} * K_{zx} * K_{xz}. \tag{9.4}$$

Or, if we write $L = \bar{L}/h$, we may compute $\bar{L} = \bar{K}_{xx} - \bar{K}_{zz}^{-1} * \bar{K}_{zx} * \bar{K}_{xz}$. We first compute $\bar{K}_{zx} * \bar{K}_{xz}$. In discretized form this becomes

$$(\bar{K}_{zx} * \bar{K}_{xz})\,(i_0, j_0) = \sum_{i,j}\sum \bar{K}_{zx}(i_0 - i, j_0 - j)\,\bar{K}_{xz}(i, j). \tag{9.5}$$

$\bar{K}_{zz}^{-1} * \bar{K}_{zx} * \bar{K}_{xz}$ is then found as the solution $\bar{M}$ of

$$\bar{K}_{zz} * \bar{M} = \bar{K}_{zx} * \bar{K}_{xz}. \tag{9.6}$$

$\bar{M}$ may be computed recursively.

Assume that $M\,(i,j)$ is known for $i < i_0$ then

$$\bar{M}(i_0, j_0) = (\bar{K}_{zx} * \bar{K}_{xz})\,(i_0, j_0) - \sum_{i<i_0}\sum_{j} \bar{K}_{zz}(i_0 - i, j_0 - j)\,\bar{M}(i, j). \tag{9.7}$$

The array

$$\bar{L}(i, j) = \bar{K}_{xx}(i, j) - \bar{M}(i, j) \tag{9.8}$$

is shown for a few values of i,j in table 13.

Table 13. The array $\bar{L}(i,j)$

i \ j	−5	−4	−3	−2	−1	0	1	2	3	4	5
0	0.000000	0.000000	0.000000	0.000000	0.000000	0.577350	0.000000	0.000000	0.000000	0.000000	0.000000
1	0.000000	0.000000	0.000000	0.000000	−0.288675	0.000000	−0.288675	0.000000	0.000000	0.000000	0.000000
2	0.000000	0.000000	0.000000	−0.057283	0.000000	0.114565	0.000000	−0.057283	0.000000	0.000000	0.000000
3	0.000000	0.000000	−0.034755	0.012227	0.034755	−0.024454	0.034755	0.012227	−0.034755	0.000000	0.000000
4	0.000000	−0.022800	0.004222	0.025471	−0.004222	−0.005344	−0.004222	0.025471	0.004222	−0.022800	0.000000
5	−0.016021	0.000005	0.019545	−0.000268	−0.003525	0.000526	−0.003525	−0.000268	0.019545	0.000005	−0.016021

We may now solve equation (9.3), $L * u_x = \tau_x$, for u_x. The resulting scheme is almost identical to that for the scalar problem described in §5. The results obtained by this method are identical to the results obtained in §8 except that u_z is no longer computed. A great saving of computation time results since we determine values of u_x only on the crack and no longer need to sum over points in the plane $z = 0$ which lie beyond the crack tips.

PHILOSOPHICAL TRANSACTIONS OF THE ROYAL SOCIETY A MATHEMATICAL, PHYSICAL & ENGINEERING SCIENCES

10. Remarks on the method of computation

In this section I shall compare the methods used in this paper with the alternative of solving (2.2) directly by a difference method in which values of u_x and u_z are determined step by step in time at a grid of points in the (x, z) plane. We shall assume, of course, that we want to find the relative displacement across the crack and not, in the first instance, to find the radiation field away from the crack.

Let the half-length of the crack be unity and assume we wish to compute the solution as far as $t = T$ assuming again that the fastest wave speed is unity. Then in the usual finite difference method we would need a grid of points in the (x, z) plane at least so large that no reflexions come back from the edge of the grid to interfere with the motion of the crack. Let N be the number of discretization steps per unit length in both the x and z directions. Then the number of grid points will be proportional to N^2T^2.

On integrating the system of difference equations up to time T we would need a number of computational operations proportional to

$$\gamma N^3 T^3, \tag{10.1}$$

where γ is the ratio of the space step size to the time step size.

In solving the problem by our method outlined in § 9 or the antiplane strain problem of § 5 we need only N space steps but in computing the solutions up to $t = T$ we should use a number of computational operations proportional to

$$\gamma^2 N^4 T^2. \tag{10.2}$$

To use our method of § 8 where values of u_z are determined on the plane $z = 0$ both on and beyond the tips of the crack the number of computational steps required is proportional to

$$\gamma^4 N^4 T^4. \tag{10.3}$$

For fixed γ and N the number of computational steps required to solve for T units of time increases most rapidly with T for our method of § 8 and least rapidly for our method of § 9 where grid points off the end of the crack were considered. The conventional method gives an intermediate rate of increase.

It is interesting to consider the values of γ which are required for stability. In the conventional computation scheme with equal steps in the x and z directions γ must be less than $1/\sqrt{2}$. The reason why we were able to take $\gamma = 1$ in our difference scheme for the integral equation is that round-off errors are introduced only on the region R and the whole system is heavily damped by the radiation of energy away from R. A more thorough numerical analysis of our scheme will not be pursued here.

We note that in three-dimensional problems the formula corresponding to (10.1), (10.2) and (10.3) are respectively

$$\gamma N^4 T^4, \tag{10.1a}$$

$$\gamma N^2 T^2, \tag{10.2a}$$

and

$$\gamma^5 N^5 T^5. \tag{10.3a}$$

Thus in three dimensions our method of § 9 has an even greater economy of computation over the other methods.

Some remarks are in order here on our method of discretizing the kernel. This is relatively time consuming since the number of operations required to compute the kernel to I time steps

is proportional to I^4. We were content to evaluate $\bar{K}$ of § 7 to forty time steps. This took about 3 min on an IBM system 360 model 67. Once computed it was stored on tape for future use. Some saving of computer time could probably have been achieved by combining our method of discretization near the apex of the array with analytical formulae when available away from the apex. In this work no attempt to minimize computer time has been made.

11. Geophysical conclusions

The solution shown in figures 16 and 17 represents, so far as a two-dimensional solution can, a fairly realistic model of a seismic source. But some improvements may be made quite simply.

The continuation for larger times of this solution would show a decrease in the tangential displacement to the static solution of (8.5). However, frictional forces are more likely to lock the crack in the configuration of its maximum relative displacement.

It is also unlikely that any real earthquake would possess such a symmetric form. For instance a plausible mechanism for triggering a shock would be creep at one end of the active fault. This would give rise to a crack nucleated from one end, that is, a unilateral crack.

It is suggested that unilateral cracks and especially three-dimensional crack models should be obtained by the method described in this paper and used to obtain a greater understanding of the generation of seismic radiation by earthquakes.

This work was carried out while the author held a research fellowship of the U.K.A.E.A. and a visiting research associateship at The Pennsylvania State University.

The author wishes to acknowledge his appreciation of the excellent computing facilities at The Pennsylvania State University.

References

Archambeau, C. B. 1968 General theory of elastodynamic source fields. *Rev. Geophys.* **5**, 241–288.

Banaugh, R. P. 1962 Scattering of acoustic and elastic waves by surfaces of arbitrary shape. Ph.D. Thesis, University of California, Lawrence Radiation Laboratory UCRL–6779 Physics, UC–34 TID–4500 (17th ed.).

Banaugh, R. P. & Goldsmith, W. 1963 Diffraction of steady elastic waves by surfaces of arbitrary shape. *Trans. Am. Soc. mech. Engrs* (E) *J. appl. Mech.* **30**, 589–597.

Ben-Menahem, A. 1961 Radiation of seismic surface waves from finite moving sources. *Bull. seism. Soc. Am.* **51**, 401–435.

Broberg, K. B. 1960 The propagation of a brittle crack. *Ark. Fys.* **18**, 159–192.

Burridge, R. & Knopoff, L. 1964 Body force equivalents for seismic dislocations. *Bull. seism. Soc. Am.* **54**, 1875–1888.

Burridge, R. & Willis, J. R. 1969 The self-similar problem of the expanding elliptical crack in an anisotropic solid. *Proc. Camb. Phil. Soc.* **66** (in press).

Craggs, J. 1966 The growth of a disc-shaped crack. *Int. J. Engng Sci.* **4**, 113–124.

Fox, E. N. 1949 The diffraction of two-dimensional sound pulses incident on an infinite uniform slit in a perfectly reflecting screen. *Phil. Trans.* A **242**, 1–33.

Friedlander, F. G. 1946 On the integrals of a partial differential equation. *Proc. Camb. Phil. Soc.* **43**, 348–359.

Friedman, M. B. & Shaw, R. 1962 Diffraction of pulses by cylindrical obstacles of arbitrary cross-section. *Trans. Am. Soc. mech. Engrs* (E) *J. appl. Mech.* **29**, 40–46.

Halliday, G. S. 1969 The stress field due to a propagating antiplane strain crack (in preparation).

Hirasawa, T. & Stauder, W. 1965 On the seismic body waves from a finite moving source. *Bull. seism. Soc. Am.* **55**, 237–262.

Kostrov, B. V. 1964*a* Self-similar problems of propagation of shear cracks. *J. appl. Math. Mech.* **28**,1077–1087.

Kostrov, B. V. 1964*b* Unsteady propagation of longitudinal shear cracks. *J. appl. Math. Mech.* **28**, 1241–1248.

Starr, A. T. 1928 Slip in a crystal and rupture in a solid due to shear. *Proc. Camb. Phil. Soc.* **24**, 489–500.

PHILOSOPHICAL TRANSACTIONS OF THE ROYAL SOCIETY A MATHEMATICAL, PHYSICAL & ENGINEERING SCIENCES

PHILOSOPHICAL TRANSACTIONS OF THE ROYAL SOCIETY A MATHEMATICAL, PHYSICAL & ENGINEERING SCIENCES

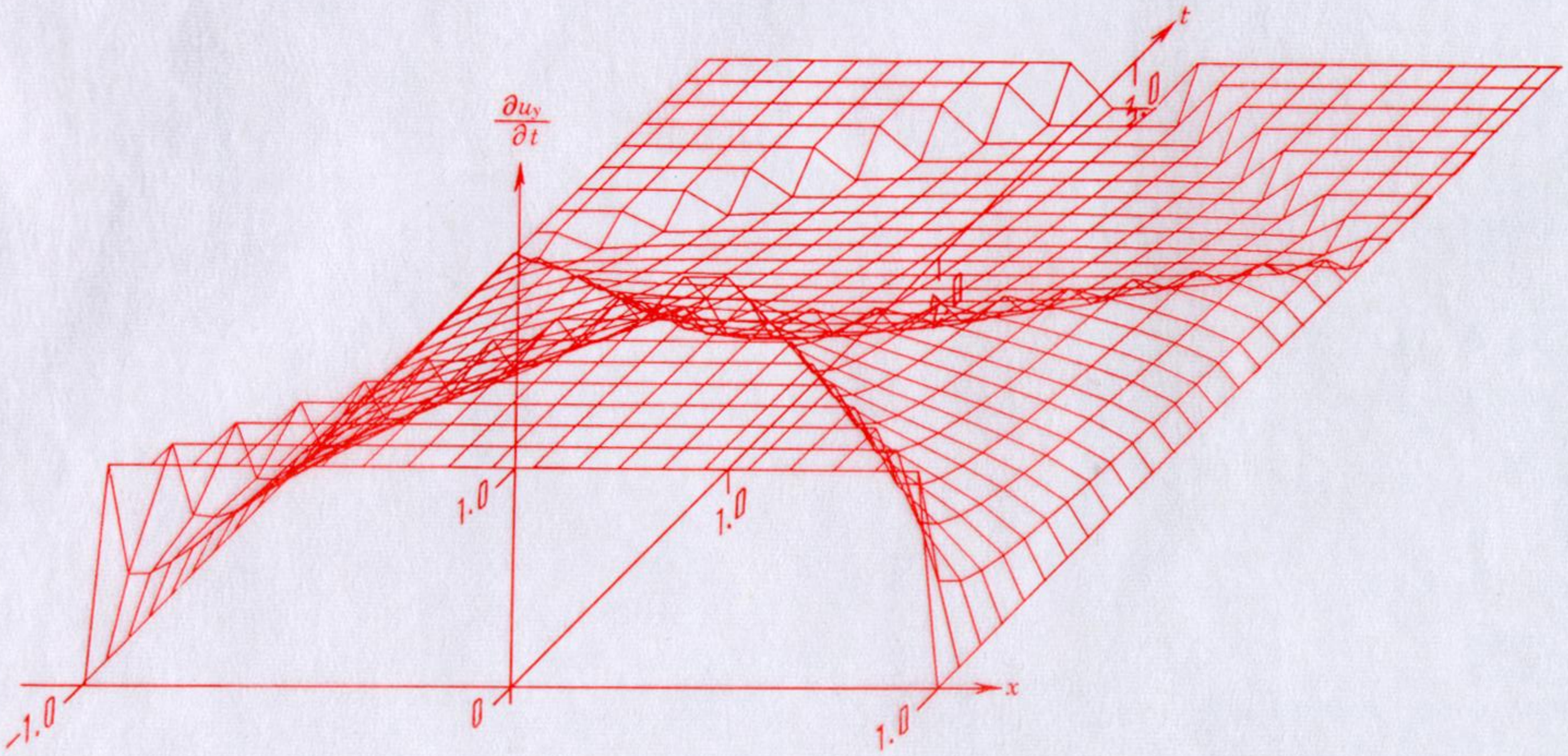

FIGURE 5. Here is shown a perspective view of the solution $\partial u_y/\partial t$ of (6.5) to (6.8) (measured vertically) for various values of t and x (measured horizontally). Beyond the region D where the solution was not computed $\partial u_y/\partial t$ was arbitrarily set to zero.

Phil. Trans. A. 265

Burridge. Overlay to figure 6, p. 364.

PHILOSOPHICAL TRANSACTIONS OF THE ROYAL SOCIETY A MATHEMATICAL, PHYSICAL & ENGINEERING SCIENCES

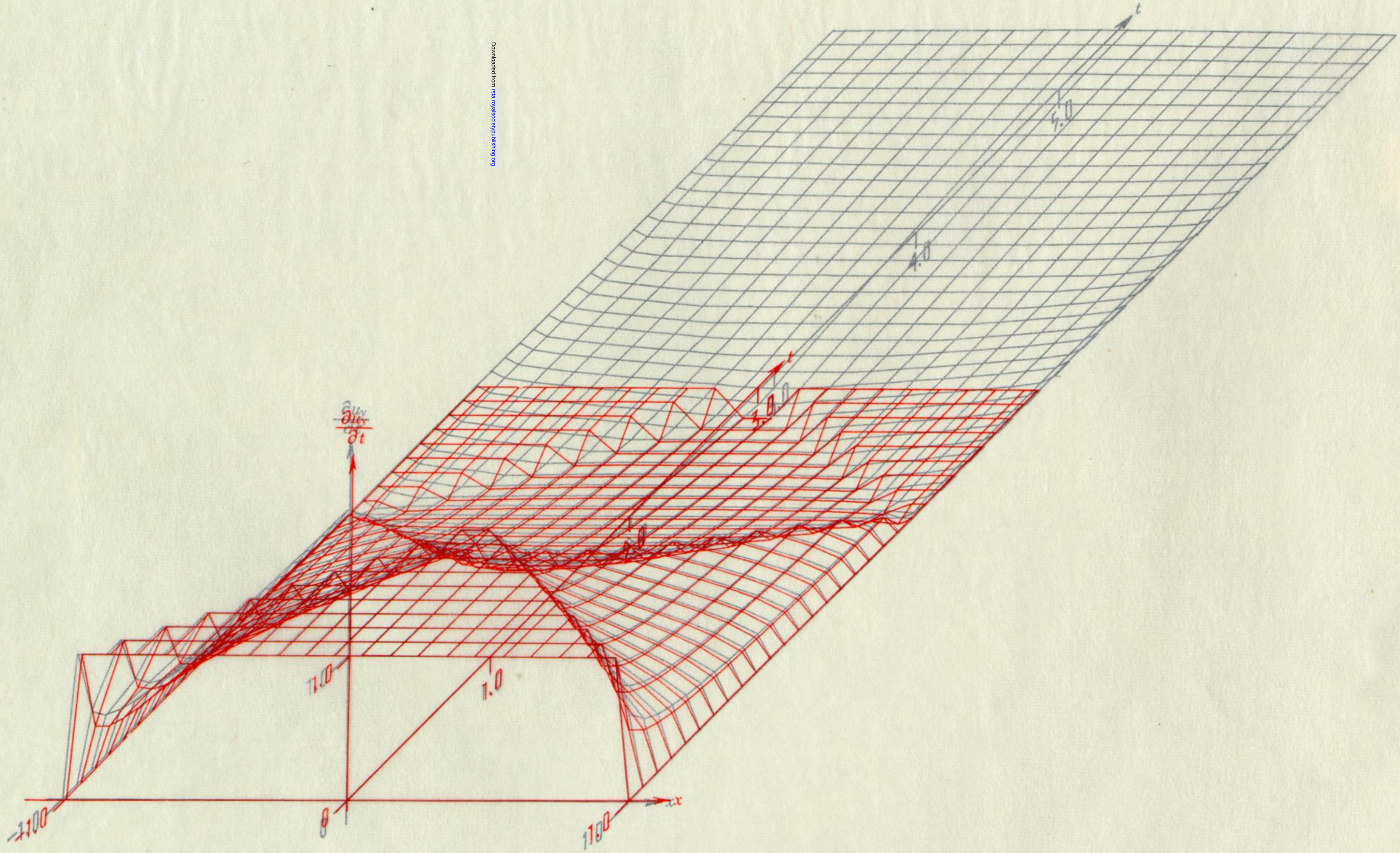

FIGURE 6. This shows the numerical solution corresponding to the analytic one shown in figure 5. We may compare the solutions as far as region D. The numerical solution is taken rather further than region D, in fact up to $t = 6$.

FIGURE 5. Here is shown a perspective view of the solution $\partial u_y/\partial t$ of (6.5) to (6.8) (measured vertically) for various values of t and x (measured horizontally). Beyond the region D where the solution was not computed $\partial u_y/\partial t$ was arbitrarily set to zero.

PHILOSOPHICAL TRANSACTIONS OF THE ROYAL SOCIETY A MATHEMATICAL, PHYSICAL & ENGINEERING SCIENCES

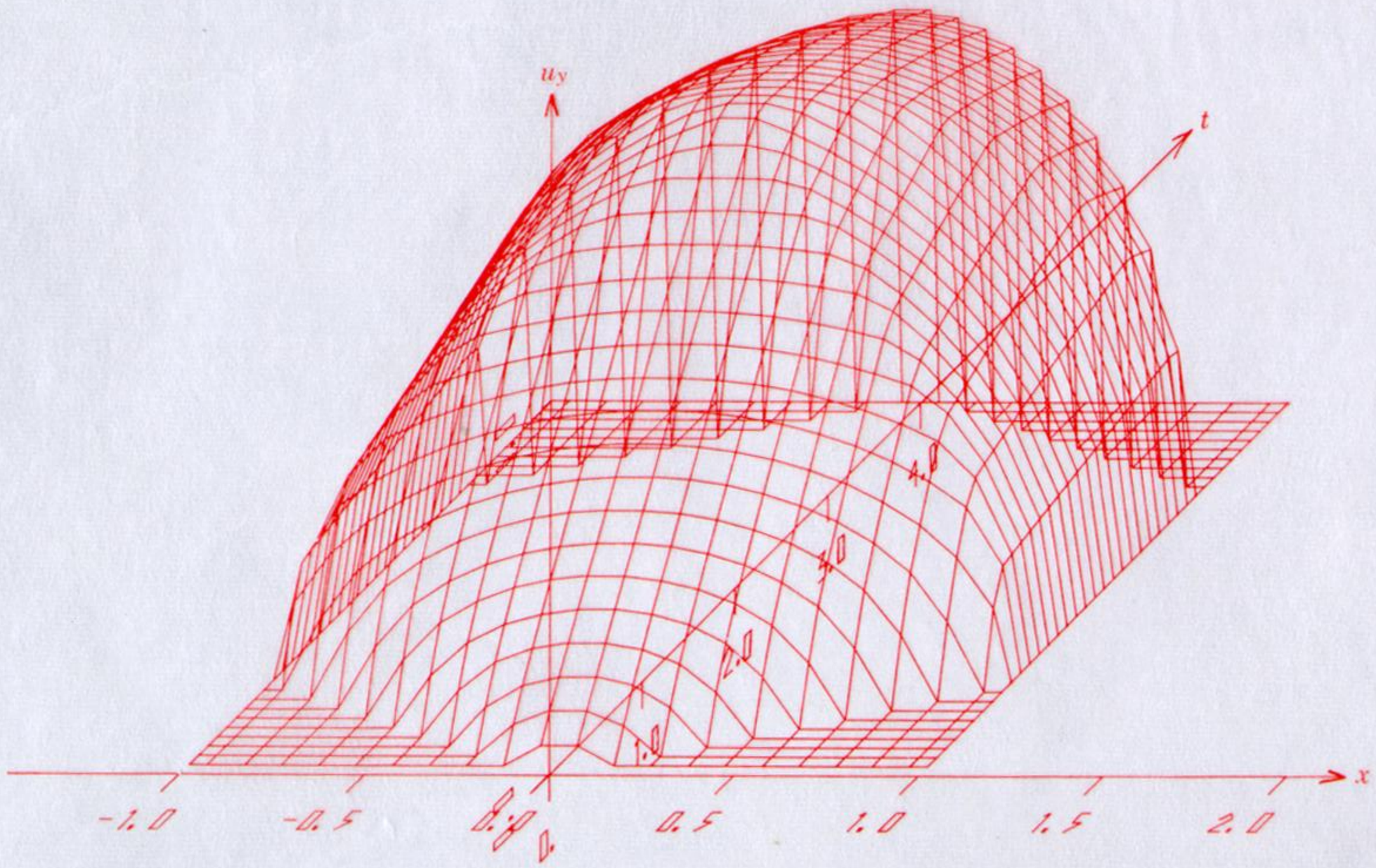

FIGURE 11. The solution of (6.11) to (6.14) is plotted as far as region D of figure 10. The value of u_y beyond region D is arbitrarily set to zero in this figure.

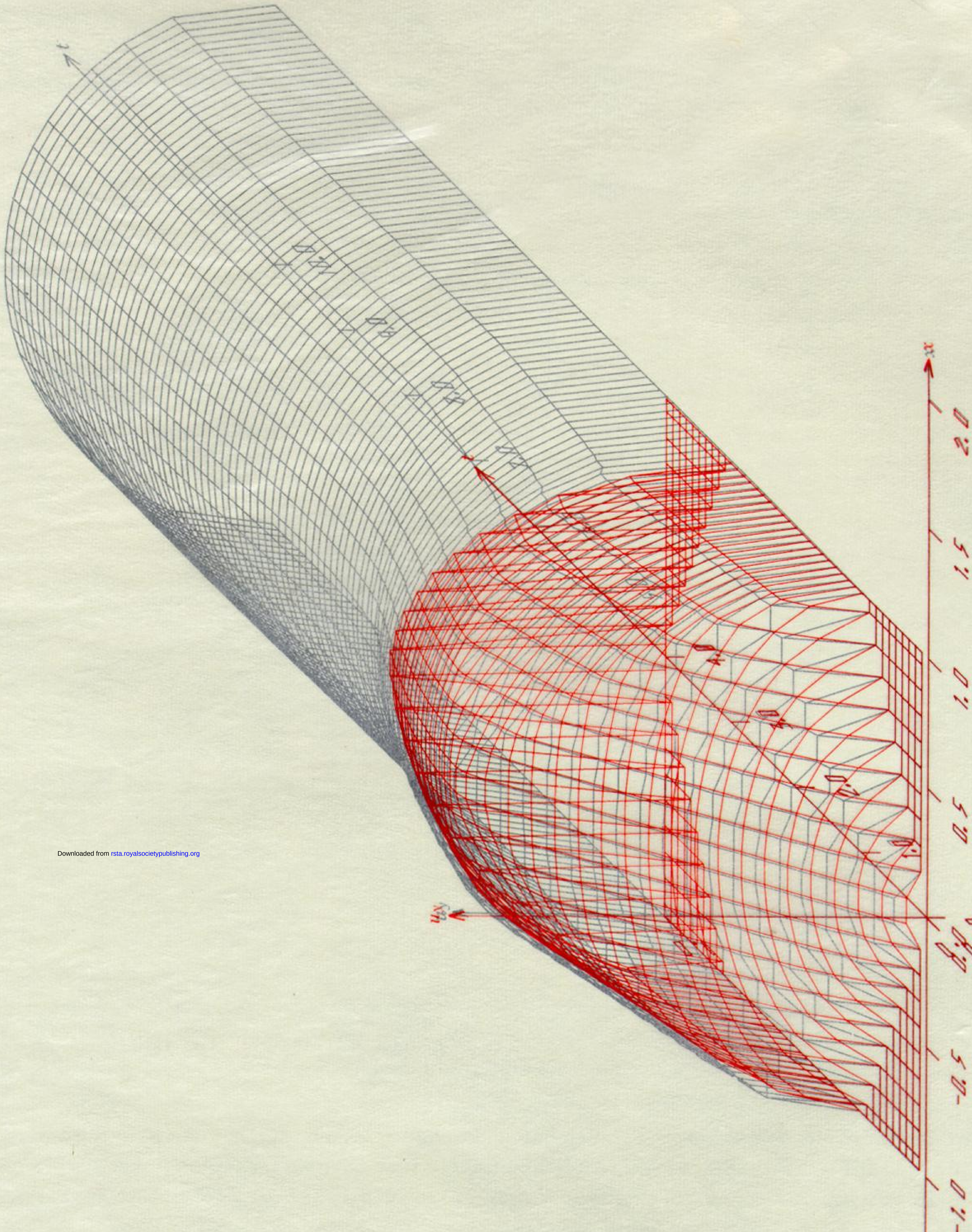

FIGURE 12. Here is shown the numerical solution corresponding to the analytic one of figure 11. It is plotted as far as $t = 10$. For (t, x) in regions A, B, C, D of figure 10 the solution shown here should be compared with that of figure 11.

FIGURE 11. The solution of (6.11) to (6.14) is plotted as far as region D of figure 10. The value of u_y beyond region D is arbitrarily set to zero in this figure.

PHILOSOPHICAL TRANSACTIONS OF THE ROYAL SOCIETY A MATHEMATICAL, PHYSICAL & ENGINEERING SCIENCES